CAS course on "Magnets", Bruges, 16 - 25 June, 2009

Physics & Measurements of Magnetic Materials III

Stefano Sgobba
EN-MME-MM
CERN

Structure and contents

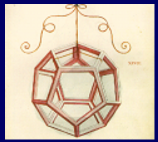

(I) Magnetic properties of materials: types of magnetic behaviour

(II) Conventional and innovative magnetic materials of interest for accelerator technology

(III) Methods of measurements

Magnetic lag

Innovative material solutions for magnets

(IV) General conclusions

Methods of measurements

1. Characterisation of soft magnetic materials
2. Measurement of feebly magnetic materials

1. Characterisation of soft magnetic materials

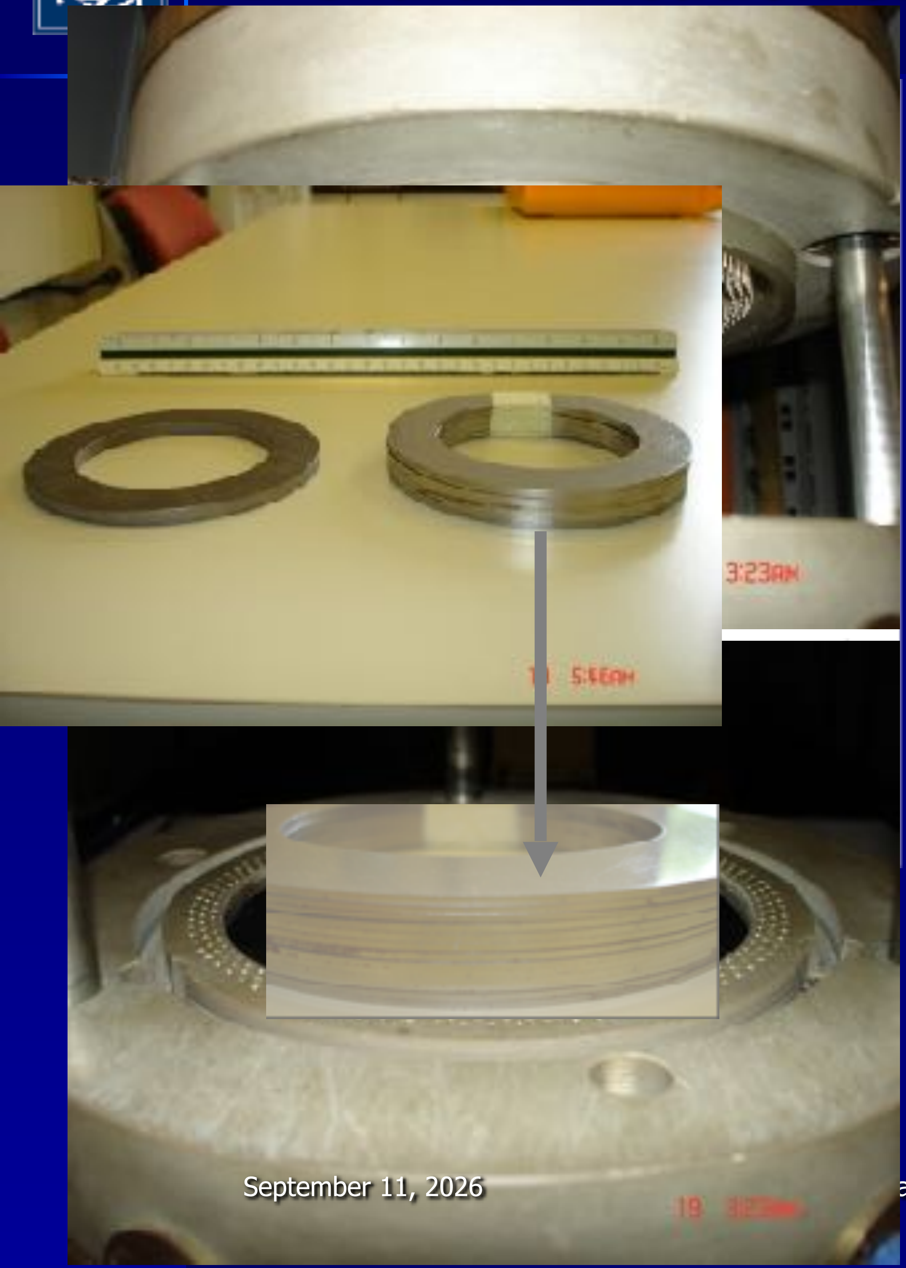

"Split-coil" permeameter available at CERN

P. Haren, Magnetic Permeability Measurements, Automatic Testing of Ring Samples at Cryogenic and Ambient Temperatures, CERN ISR-BOM/78-4

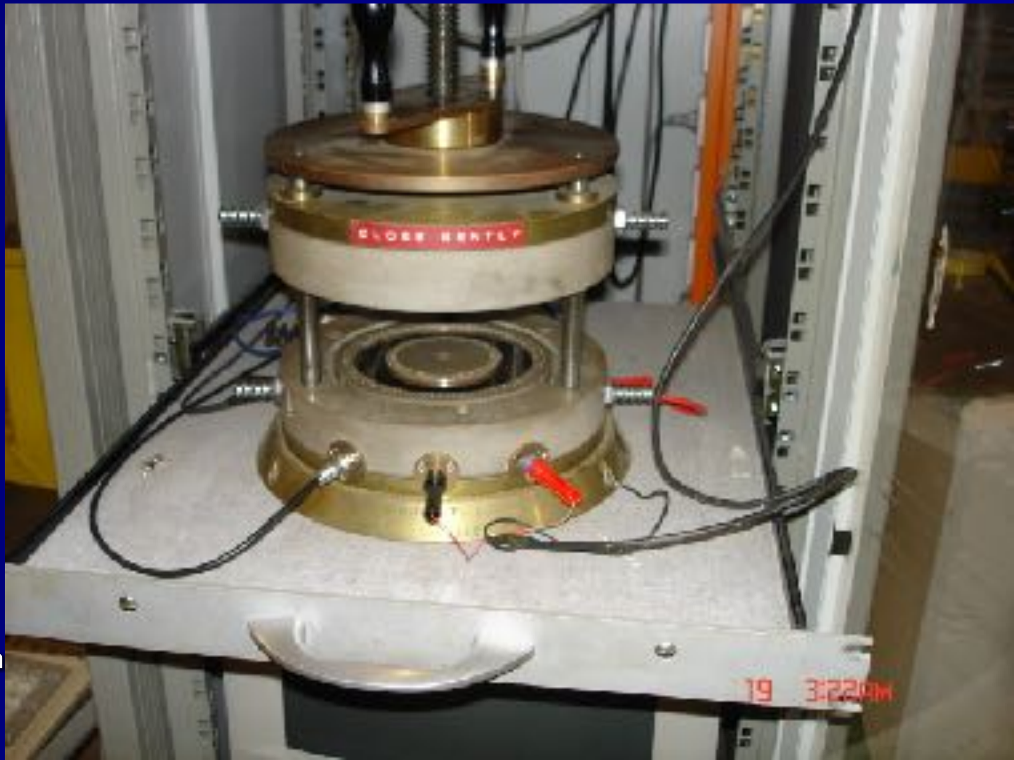

1. Characterisation of soft magnetic materials

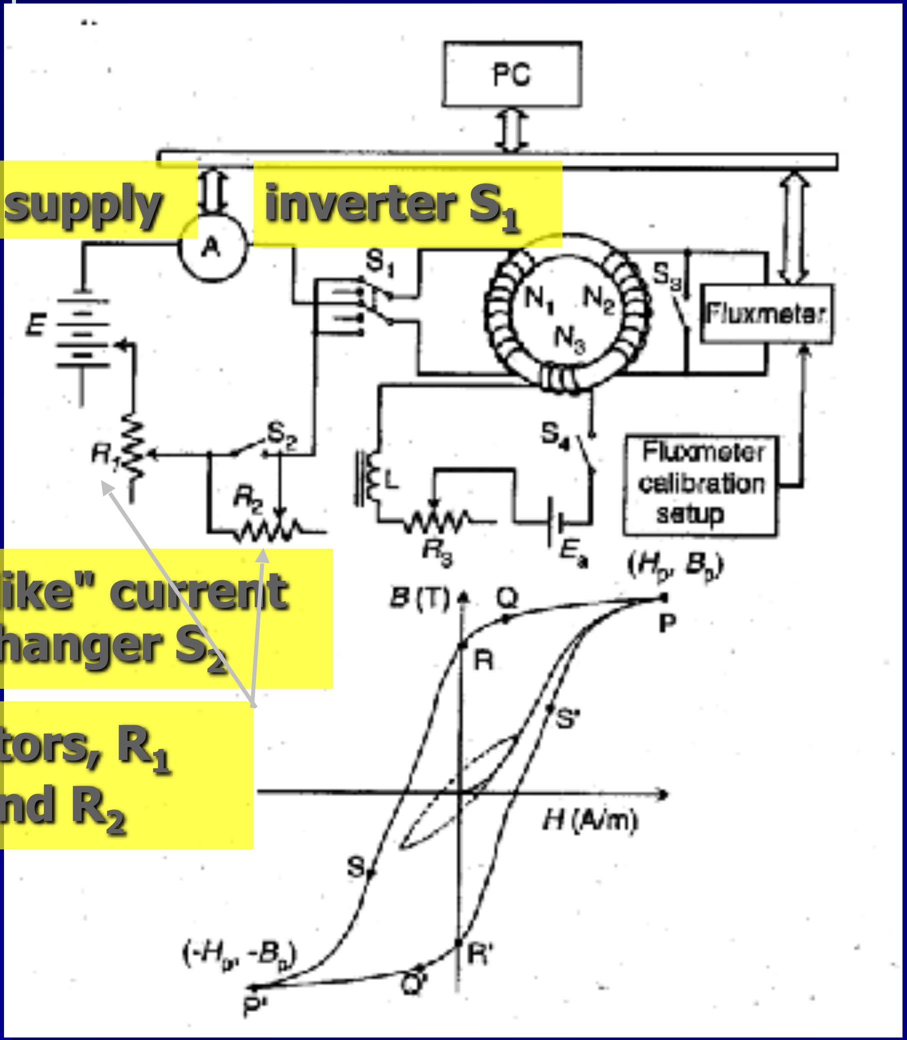

power supply

inverter S_1

"step-like" current changer S_2

regulators, R_1 and R_2

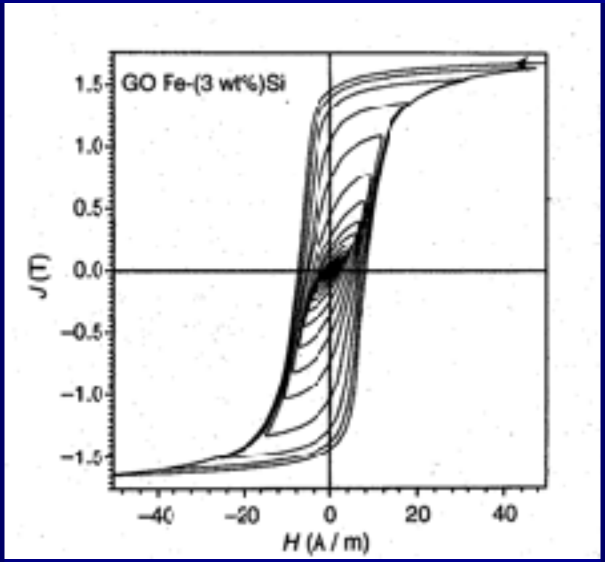

DC: every recorded point should correspond to a stable microscopic configuration of the system

F. Fiorillo, Characterization and Measurement of Magnetic Materials, Elsevier, 2004

1. Characterisation of soft magnetic materials

- Transient voltage induced on a secondary winding by a step-like field variation
- Integrated over a time interval for complete decay of eddy currents
- Need of a reference condition ("flux variations")
- Saturated (or demagnetised state)

1. Characterisation of soft magnetic materials

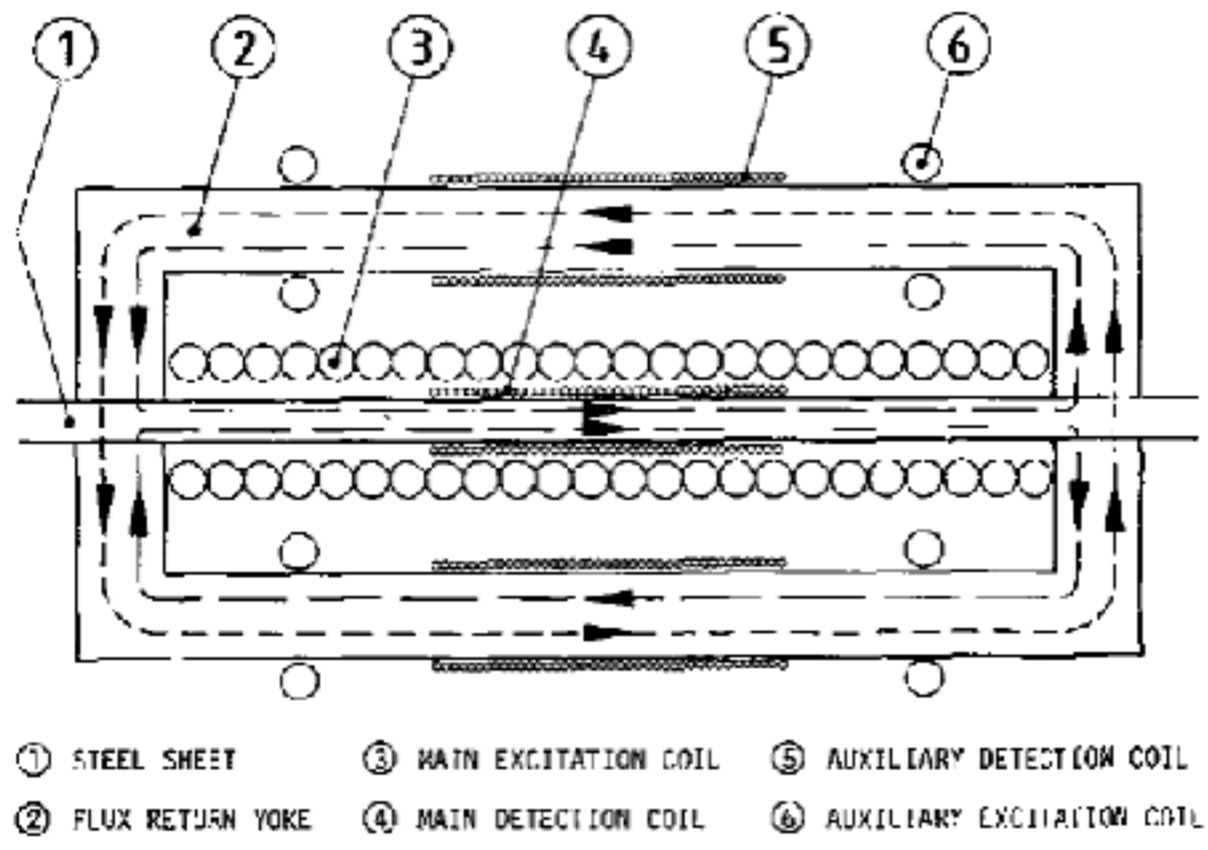

Fig. 1 - Schematic cross-section of the coercimeter

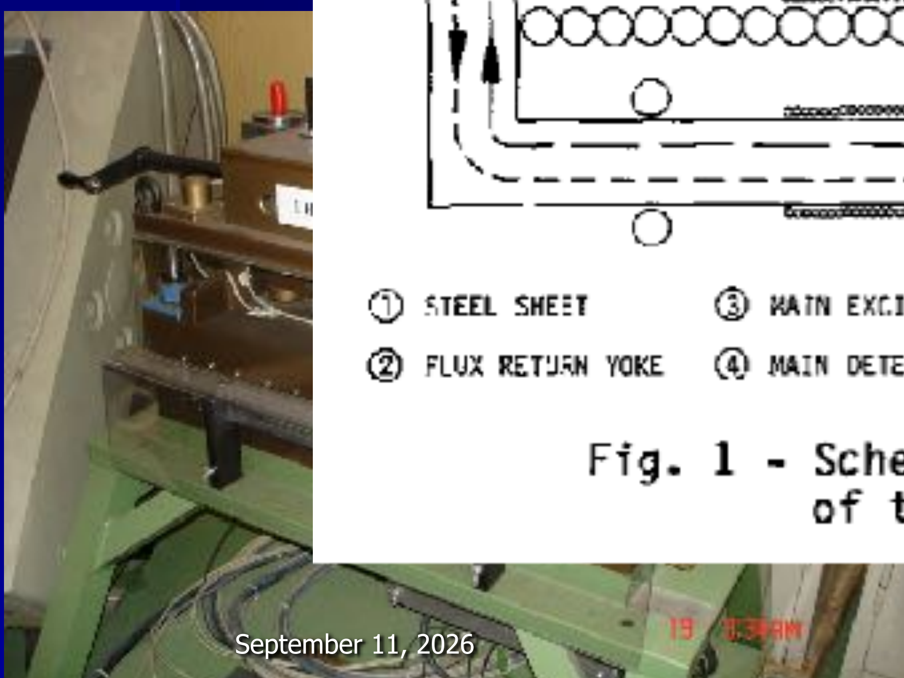

Destructive
of Steel
Sheets, Journal de Physique Colloques 45, C1 (1984) C1-965-C1-968

Jinst
PUBLISHED BY INSTITUTE OF PHYSICS PUBLISHING AND SISSA
RECEIVED: *November 21, 2006*
REVISED: *February 15, 2007*
ACCEPTED: *March 19, 2007*
PUBLISHED: *March 21, 2007*

TECHNICAL REPORT

oft magnetic materials

Electromagnetic characterization of the 990 ton gapless magnets for the OPERA experiment

A. Cazes,[a] A. Cecchetti,[a] B. Dulach,[a] F. Iungo,[a] M. Incurvati,[a] D. Orecchini,[a] G. Peiro,[b] C. Sanelli,[a] F. Terranova[a*] and M. Ventura[a]

[a] *Laboratori Nazionali di Frascati dell'INFN, Frascati (RM), Italy*
[b] *CERN, Geneve, Switzerland*

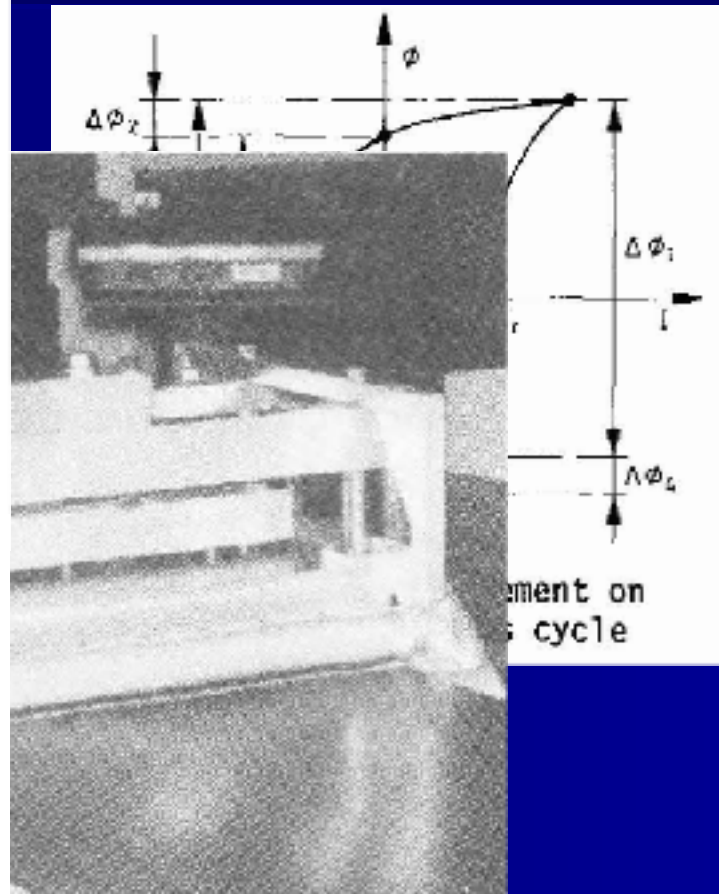

tion of a sheet
percimeter

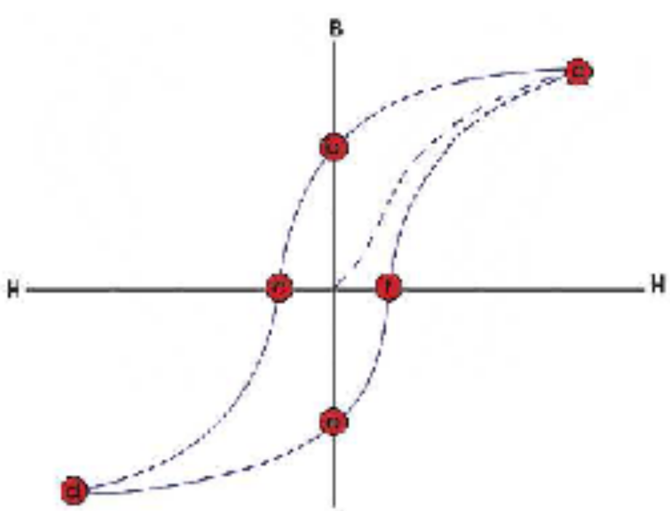

Figure 5. Paths used to measure the magnetic fi eld with the ramp-up technique.

2. **Measurement of feebly magnetic materials**

- ✓ Measurement of material permeabilities in the range μr = 1.00001 to 2 (4)
- ✓ Permeability measurements with results that can be traced to national standards

Courtesy of Foerster, MAGNETOSCOP® 1.069

- Measurement of material permeabilities
- Materials to be measured should be thicker than 8 mm
- Measurements of materials thinner than 8 mm by stacking two pieces
- Air gap between two pieces as small as possible
- Flat area not less than 20 mm in diameter
- Radius of curvature not be less than 40 mm
- Otherwise permeability less than actual value

2. **Measurement of feebly magnetic materials**

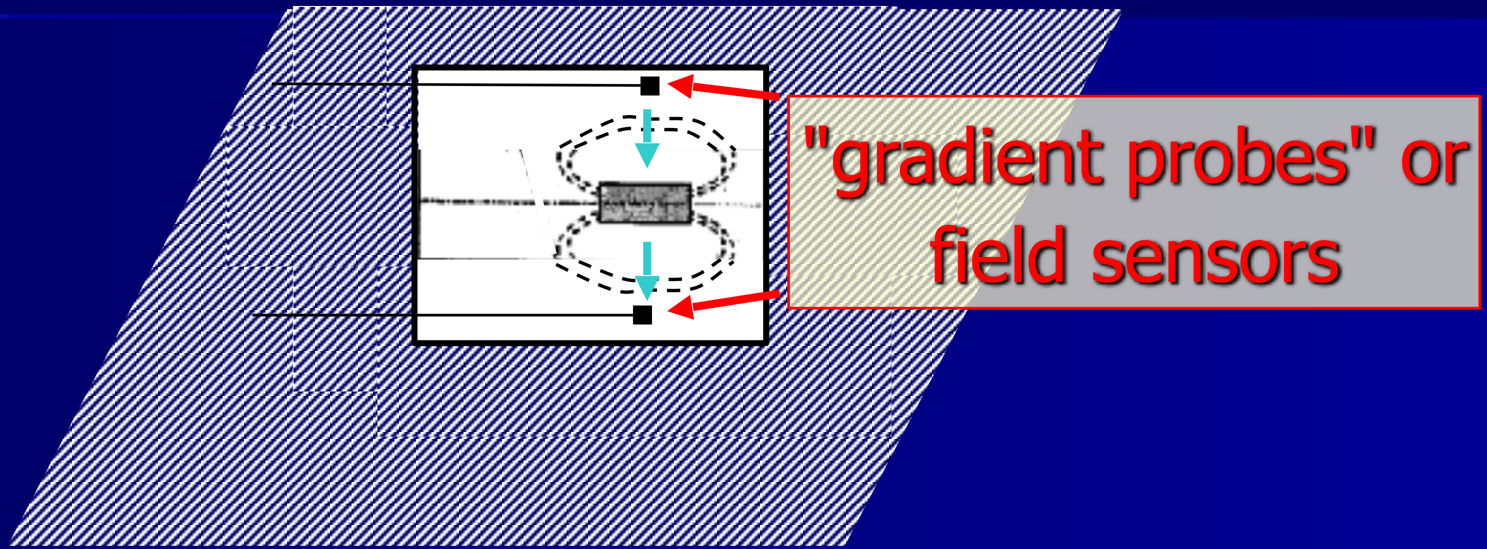

- "Based on a cylindrical permanent magnet
- A gradient probe is placed on either side of the cylindrical magnet in the plane perpendicular to the cylinder axis at the center of the permanent magnet
- If the cylindrical magnet is placed on a material whose permeability is greater than 1, there is a minute displacement of the magnetic zero of the cylindrical magnet towards the material on which the magnet has been placed
- In the lower permeability ranges this displacement is a measure of the permeability of the material"

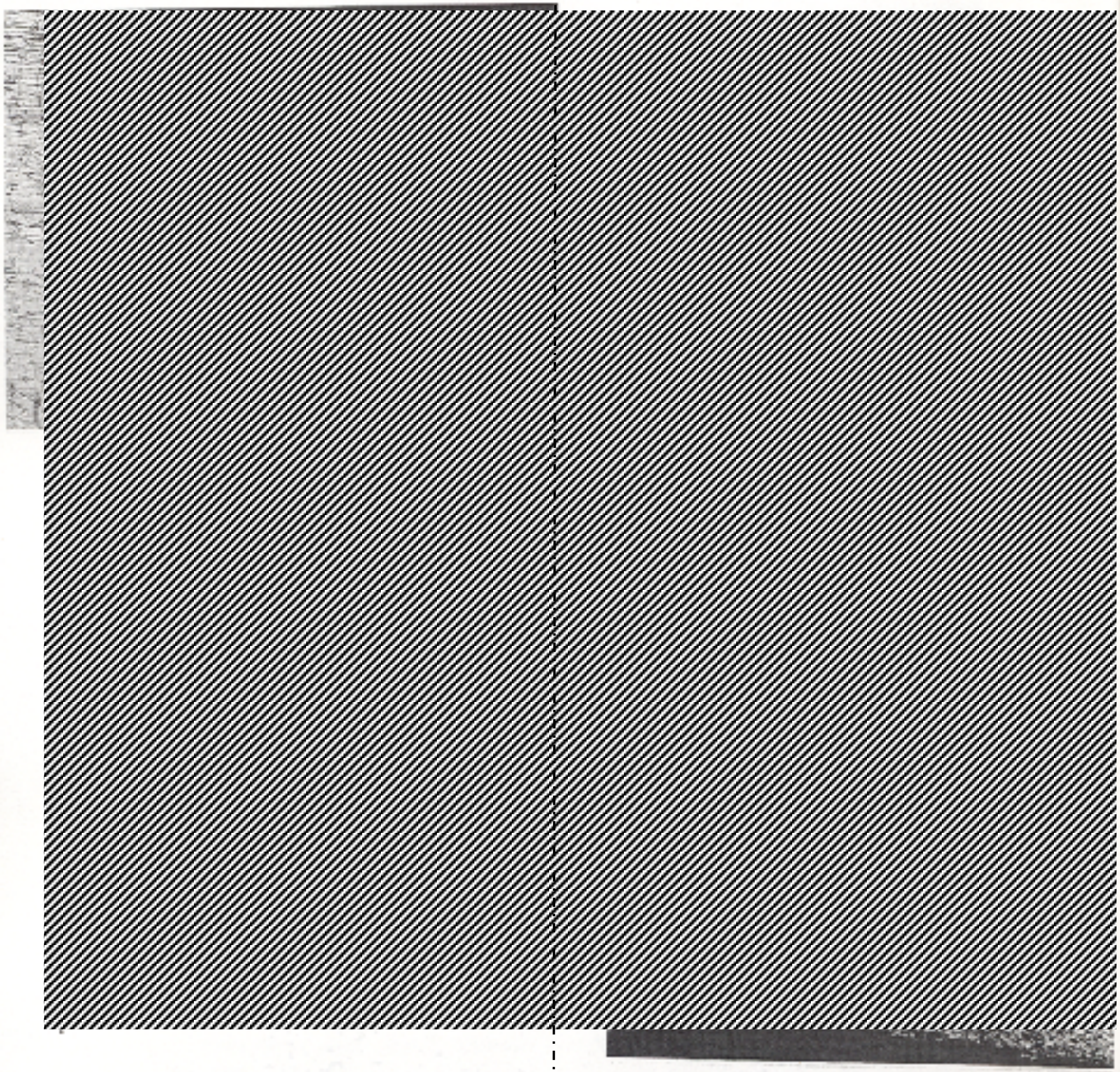

Fig. 3 : HAZ of the steel UNS 21904, welded under 15% N_2 (speed : 100 cm/min)

Fig. 3 : Microstructure (ZAT) relative à l'acier UNS 21904, soudé sous protection de 15% N_2, à la vitesse de 100 cm/min.

J.P. Bacher and S. Sgobba, TIG Weldability of Special Stainless Steels for the Beam Screen of the Large Hadron Collider, Bulletin du Cercle d'Etude des Métaux, **XVI**, p. 13.1 (1995)

…of feebly

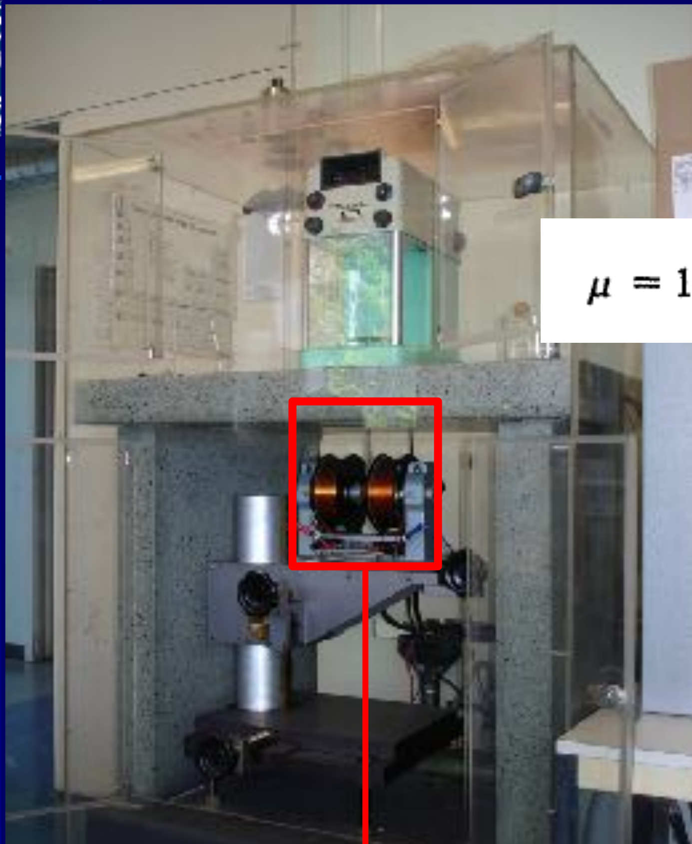

$$\mu = 1 + \frac{24.65 \Delta m}{AH^2}$$

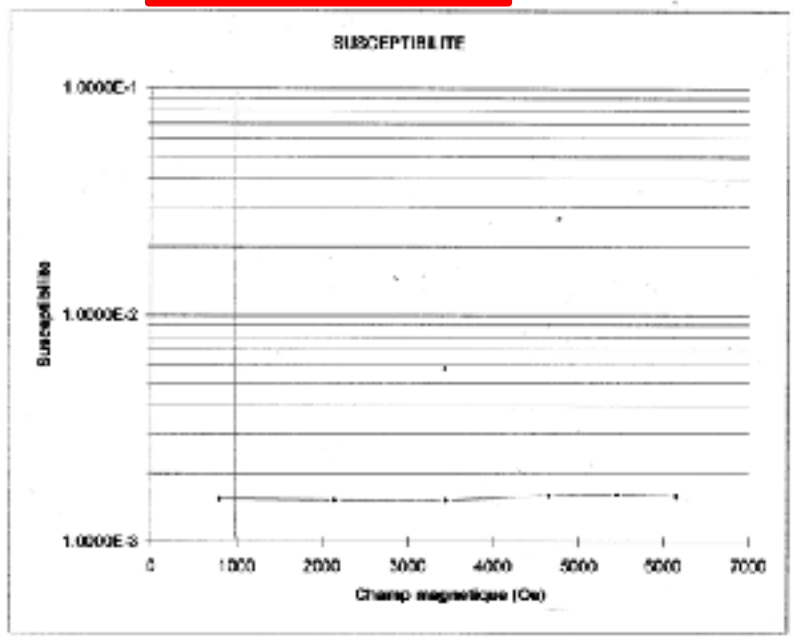

SUSCEPTIBILITE MAGNETIQUE
A 293 K

Echantillon n°:	1	Acier type :	C65072
	7.0	titre :	MOYEN
Poids (g):	0.0694	volume (mm3):	6.8974E+0
		REQUERANT:	930888A/S

INTENSITE (A)	CHAMP (Oe)	POIDS (g)	SUSCEPTIBILITE
0		25.9647	
0.2	800	25.6652	1.5566E-3
0.6	2150	25.6684	1.4308E-3
1	3450	25.6844	1.5253E-3
1.4	4650	25.6722	1.5991E-3
1.8	5450	25.6782	1.6184E-3
2.2	6150	25.6849	1.5085E-3

Susceptibilité à 1000 Oe = 1.5527E-3

S_1 - SPST Switch

S_2 - Reversing Switch

A - Ammeter

R - Rheostat

FIG. 2 Circuit Diagram for Method No. 2

2. **Measurement of feebly magnetic r**

Commercial AISI 316 austenitic stainless steel, annealed at 1400 K

AFM ⇒

MFM ⇒

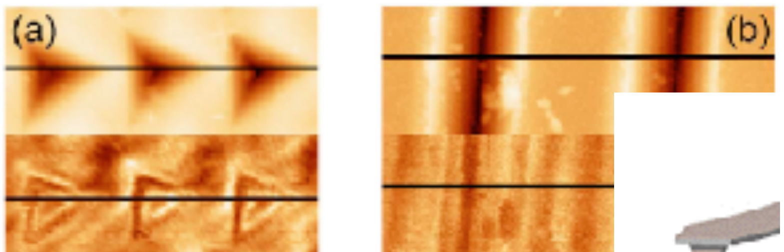

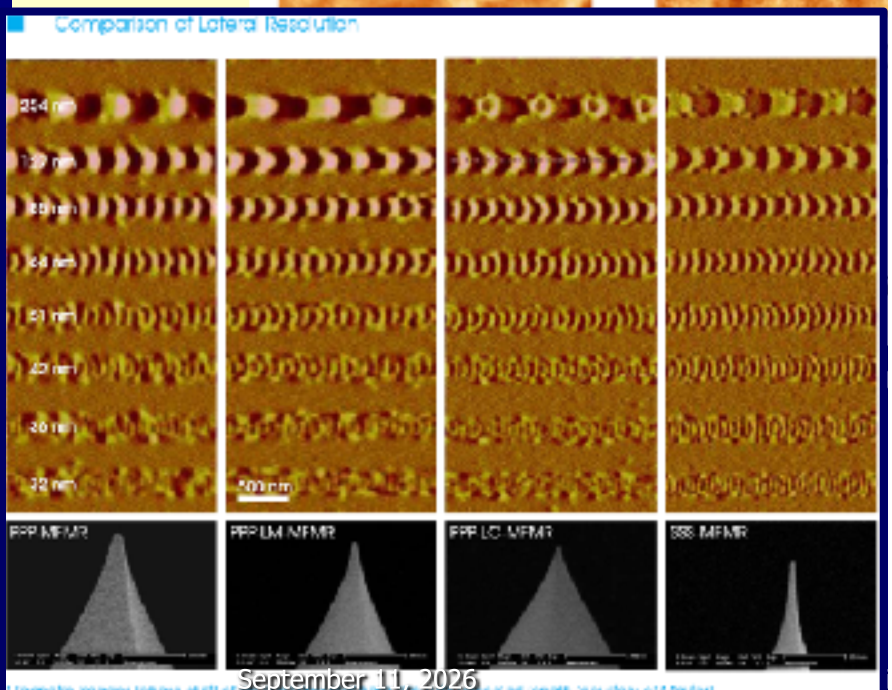

Appl. Phys. Lett. 89, 032500 (2006)

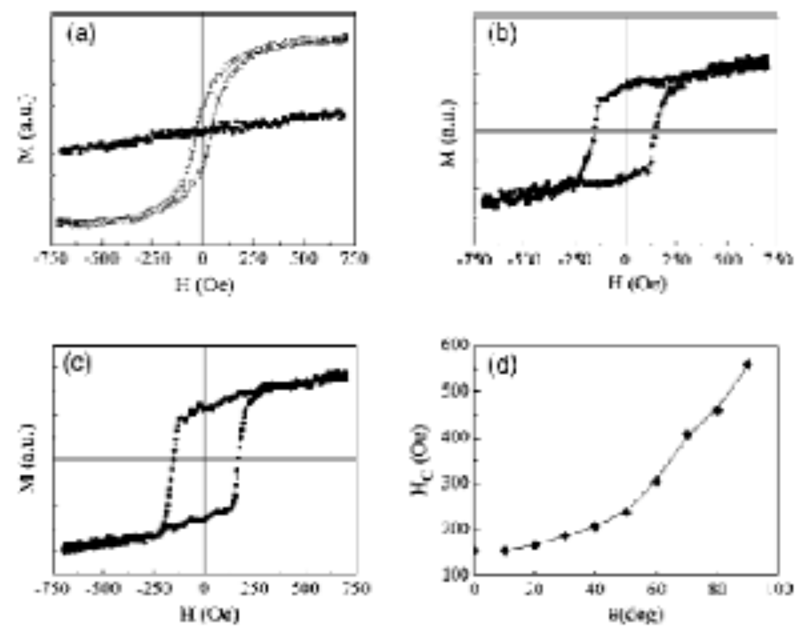

FIG. 3. (a) Hysteresis loop (□) obtained after cutting and polishing (before annealing) the austenitic stainless steel, together with the linear relationship (-●-) observed between the magnetization and the applied field after annealing the steel at 1400 K for 30 min. (b) Hysteresis loop corresponding to the array of indentations with lateral size of 1 μm. (c) Hysteresis loop obtained from the array of lines (1.8 μm wide) measured along the direction of the lines. (d) Dependence of the coercivity H_C on the angle of measurement for the array of 1.8 μm wide lines. The lines are guides to the eyes.

Source: NANOSENSORS™, Neuchâtel/ CH

Source: Veeco Instruments Inc.

2. Measurement … etic materials

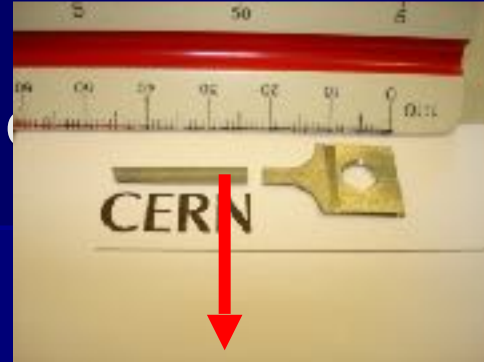

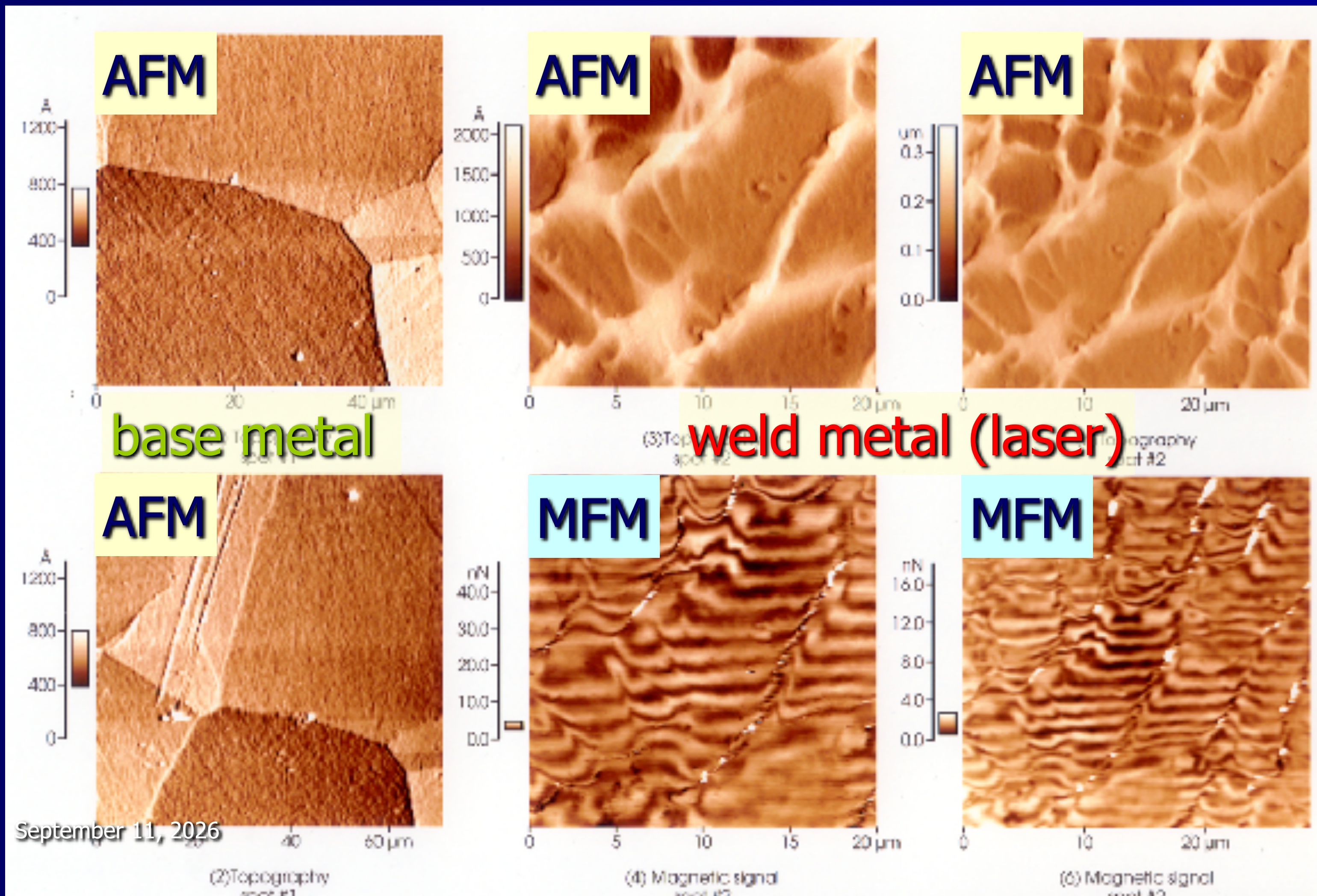

Magnetic lag

Two sources of magnetic lag:

1. lag due to eddy currents

2. magnetic
   dependen

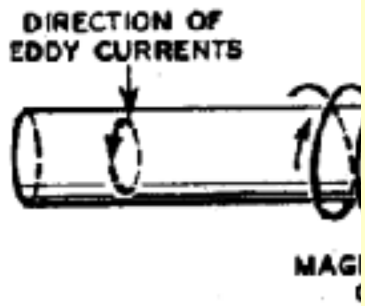

FIG. 17–1. Direction
rents in solid bar is
that of the applied
current giving ris

From Bozorth,
Ferromagne

Flow opposite to magnetising coil

Net effect:

- DC, they prevent the field from penetrating immediately to the interior of the material
- AC, "field strength in the interior may be never more than a small fraction of the field strength at the surface"

Magnetic lag

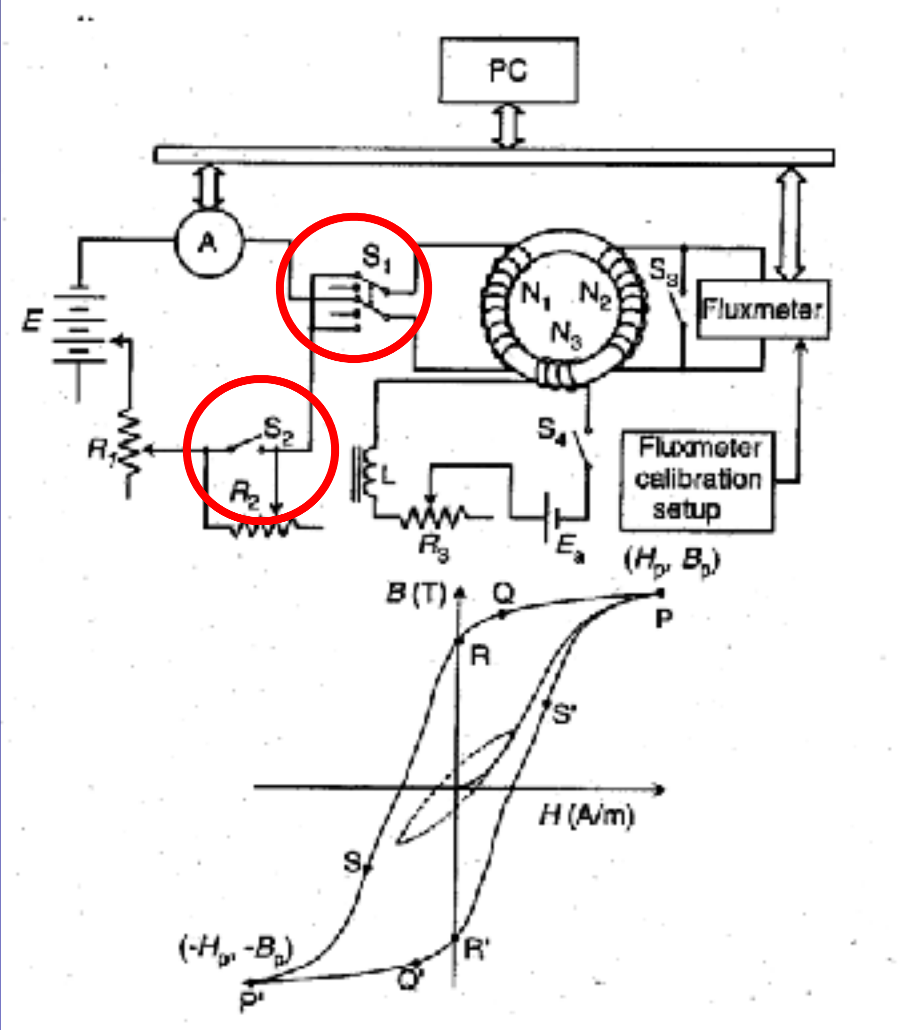

F. Fiorillo, Characterization and Measurement of Magnetic Materials, Elsevier, 2004

Sudden application of a field to a cylinder of field-dependent permeability of diam. d

$$\tau = 0.55 d^2/\rho \int dB/dH \, db/b$$

where $b = 1 - B/B_o$, B_0 is the ultimate field and ρ is the resistivity

Measurement of a lamination of rel. permeability μ_r, conductivity σ, thickness d:

$$\tau = \mu_0 \mu_r \sigma d^2/8$$

10 mm pure Fe, $\mu_r = 1000$:

$$\tau \approx 0.15 \text{ s}$$

Magnetic lag

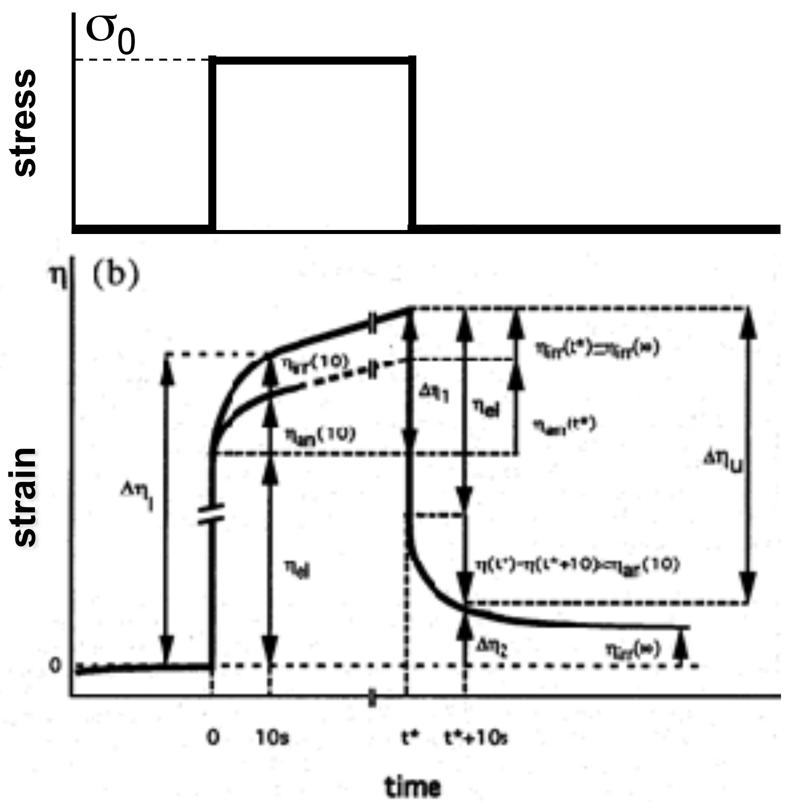

Fig. 1. (a) Load–unload cycle of a Cu-electroplated sample of Al 2024. A part of the displacement cumulated during loading remains unrelaxed. (b) Schematic representation of the different contributions to the measured displacement s (see text).

Anelastic "after-effect"

Sgobba et al., Acta Met. **43** (1995) 1171-1181

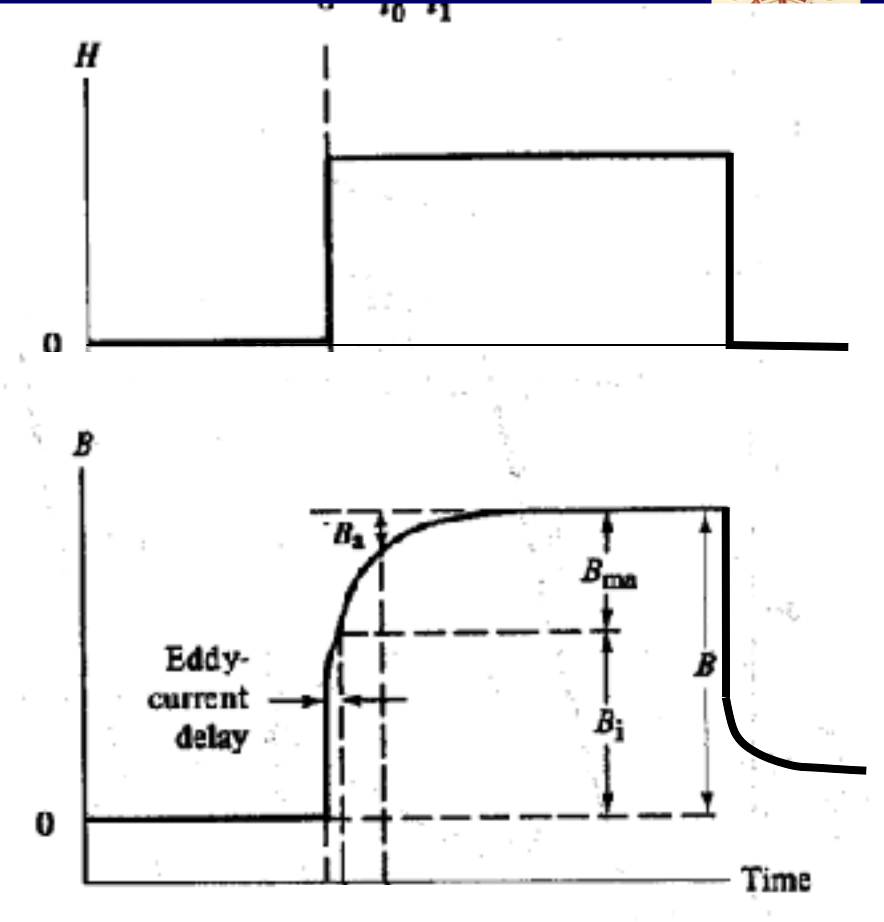

Magnetic "after-effect"

B.D. Cullity, C.D. Graham, Introduction to Magnetic Materials, 2nd ed., Wiley (2009)

Magnetic lag

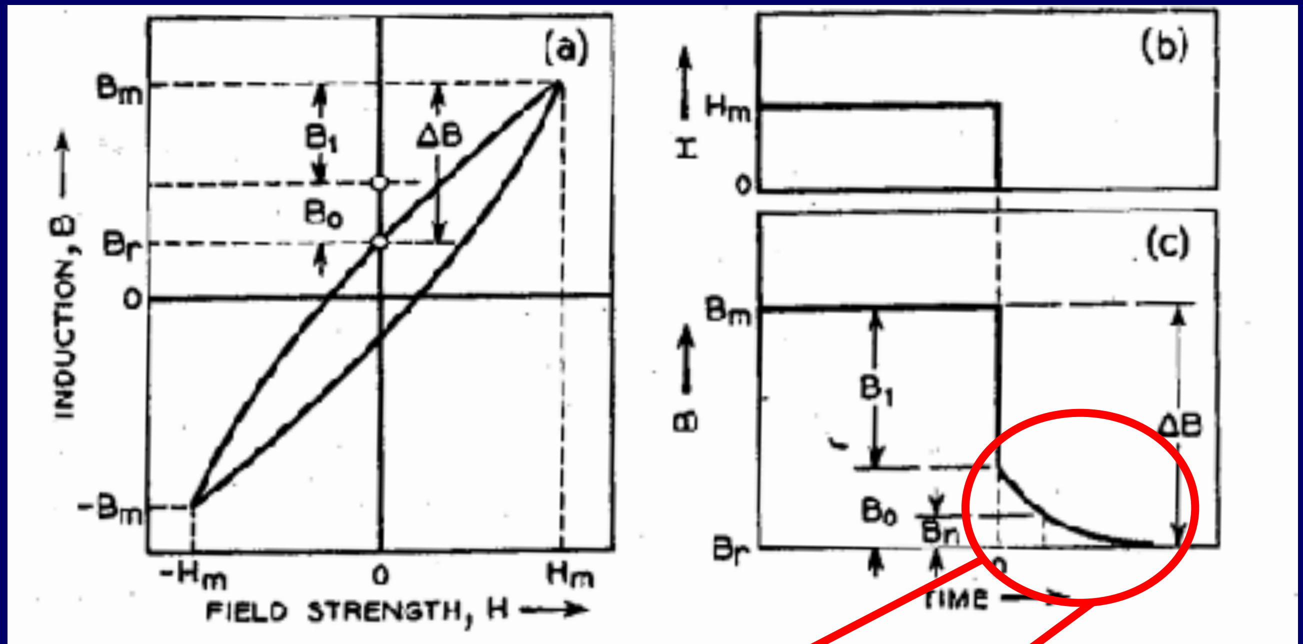

FIG. 17-11. Concepts used in the description of magnetic lag.

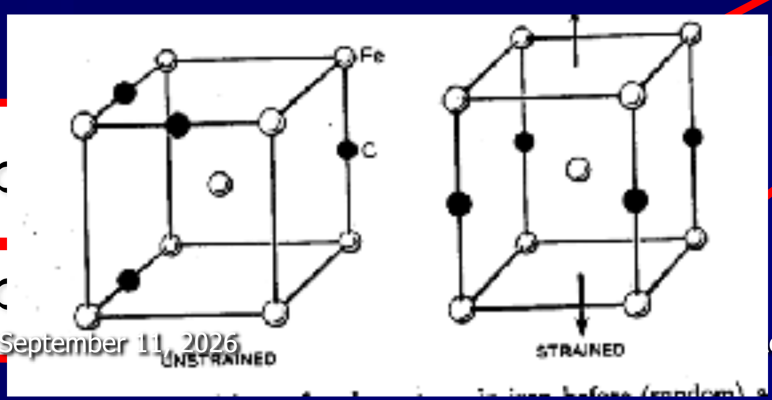

From Bozorth,
Ferromagnetism, 1951

Magnetic lag

SL-Note-2001-013 MD
20, février 2001

Mesure de l'influence magnétique du cycle proton 450 Gev sur le cycle positron

C.Arimatea, D.Jacquet

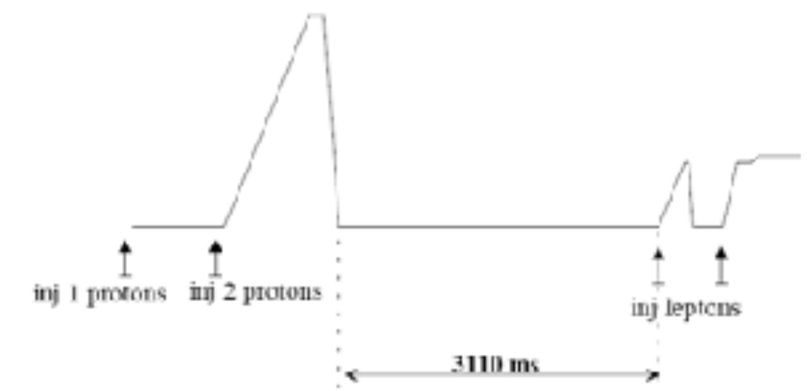

figure 3

3. Interprétation

4. Conclusion

Les effets magnétiques observés sont mal connus et d'une importance non négligeable par rapport aux champs magnétiques rémanents. Il est difficile de trouver une ressemblance entre les courbes de correction des MPS et les courbes calculées d'après nos mesures, en effet pendant la RAMP ces corrections compensent aussi d'autres effets comme le retard des alimentations ou les effets du passage de la transition. Une étude plus approfondie doit être envisagée pour mieux comprendre ces effets et les quantifier. Ils devront être pris en compte à l'avenir pour le multicycling.

Structure and contents

(I) Magnetic properties of materials: types of magnetic behaviour

(II) Conventional and innovative magnetic materials of interest for accelerator technology

(III) Methods of measurements

Magnetic lag

Innovative material solutions for magnets

(IV)
- (a) "Non-magnetic" materials, phase stability and phase transformations: LHC beam screen
- (b) Powder metallurgy applied to structural materials: end covers of LHC dipole magnets

LHC DIPOLE : STANDARD CROSS-SECTION

CERN AC/DI/MM - HE107 - 30 04 1999

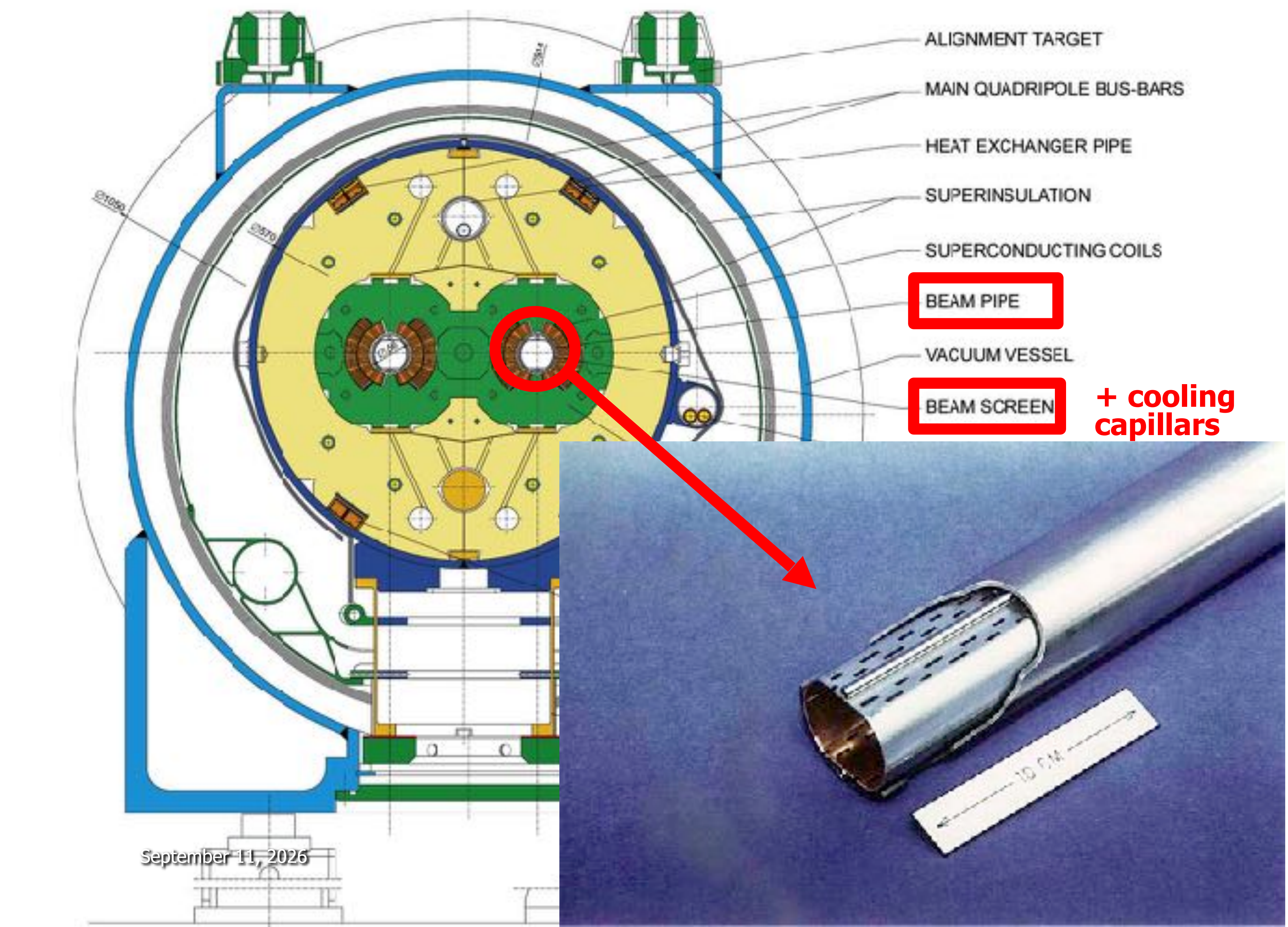

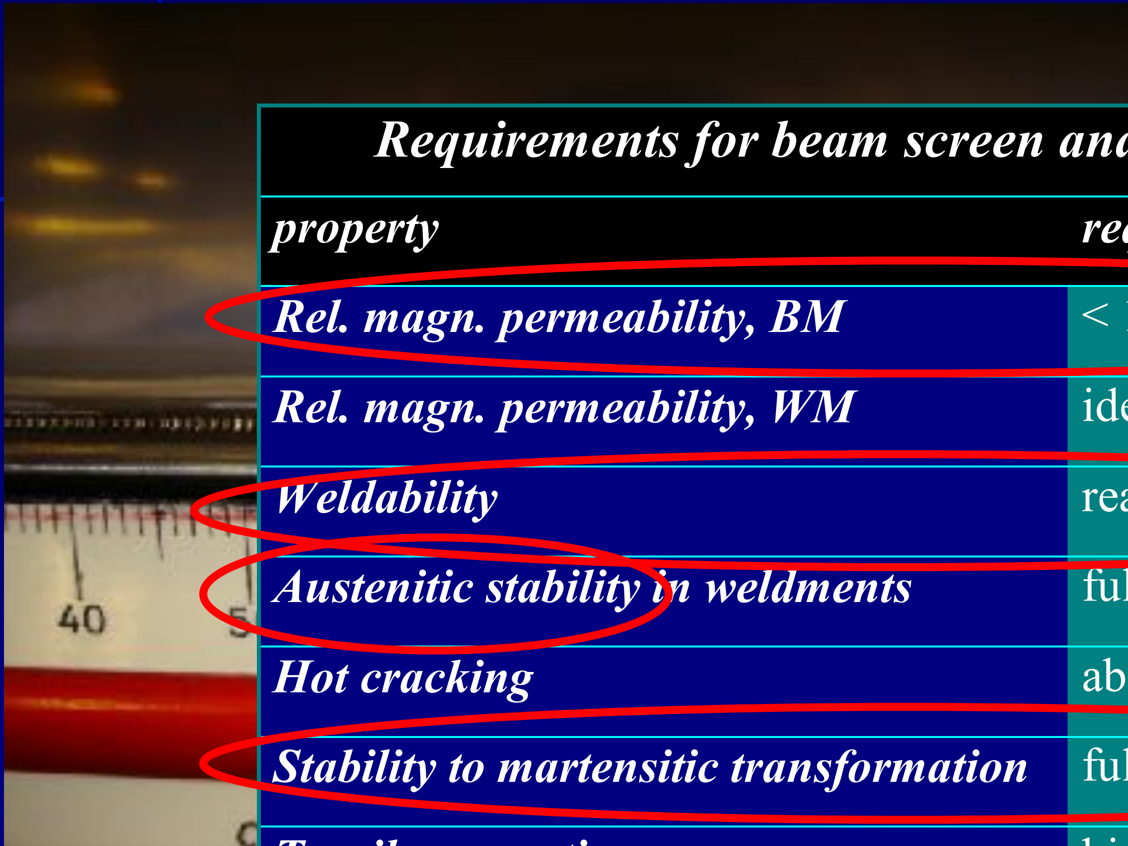

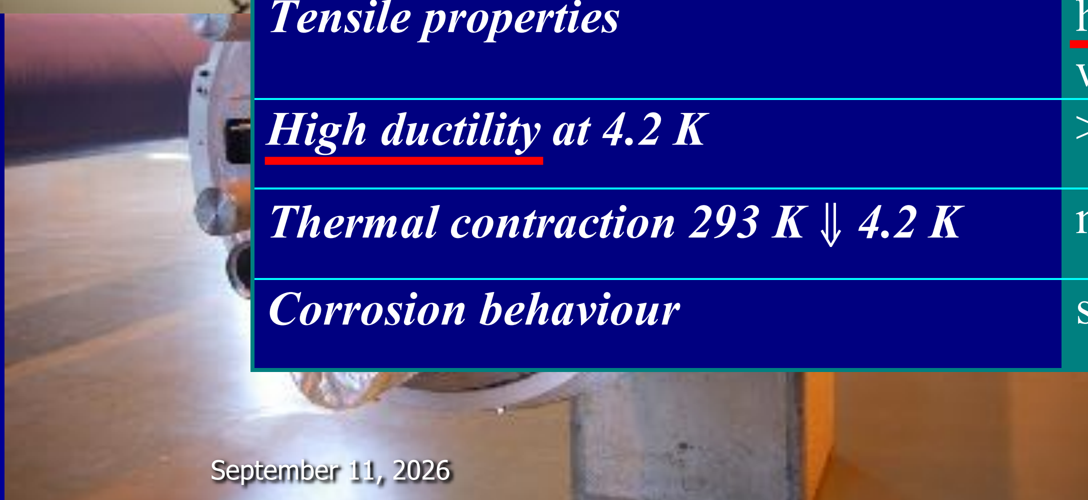

Requirements for beam screen and capillary steel

property	*requirements*
Rel. magn. permeability, BM	< 1.005 at 10K<T<20K
Rel. magn. permeability, WM	idem
Weldability	readily weldable
Austenitic stability in weldments	full
Hot cracking	absence
Stability to martensitic transformation	full
Tensile properties	high strength at RT and working T
High ductility at 4.2 K	> 200 J
Thermal contraction 293 K ⇓ 4.2 K	not far from 316LN
Corrosion behaviour	see 304L/316L

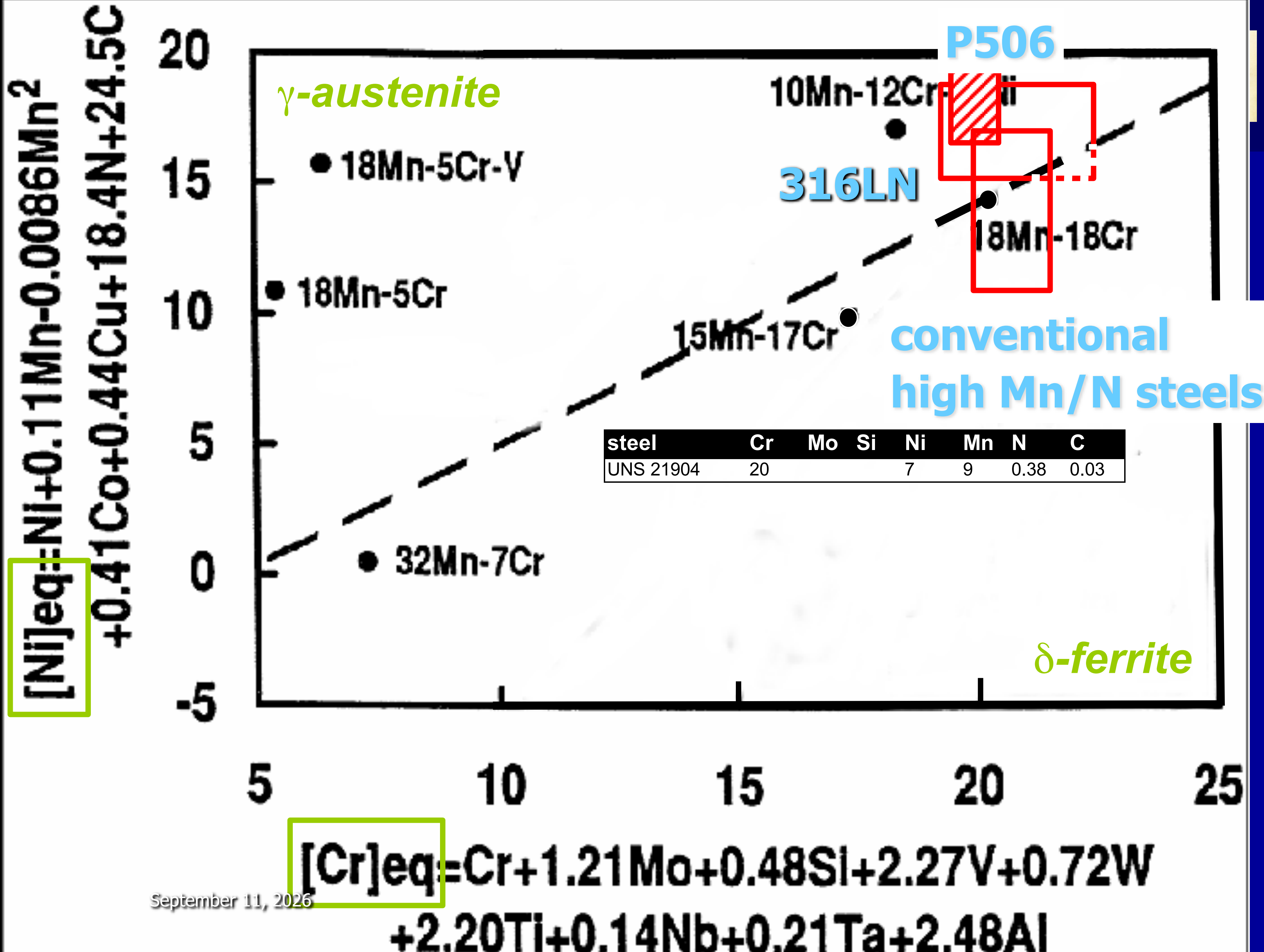

steel	Cr	Mo	Si	Ni	Mn	N	C
UNS 21904	20			7	9	0.38	0.03

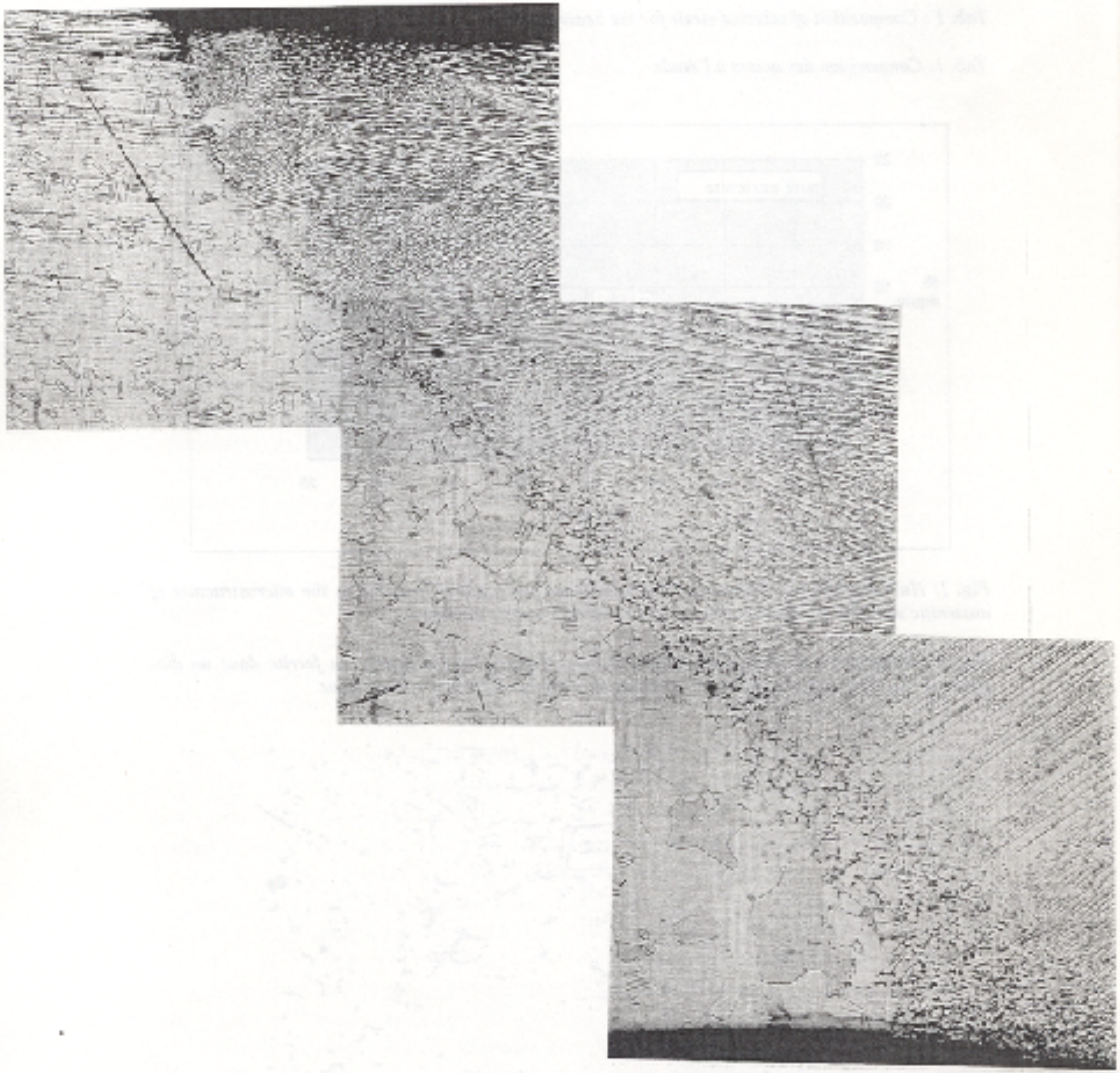

Fig. 3 : HAZ of the steel UNS 21904, welded under 15% N_2 (speed : 100 cm/min)

Fig. 3 : Microstructure (ZAT) relative à l'acier UNS 21904, soudé sous protection de 15% N_2, à la vitesse de 100 cm/min.

J.P. Bacher and S. Sgobba, TIG Weldability of Special Stainless Steels for the Beam Screen of the Large Hadron Collider, Bulletin du Cercle d'Etude des Métaux, **XVI**, p. 13.1 (1995)

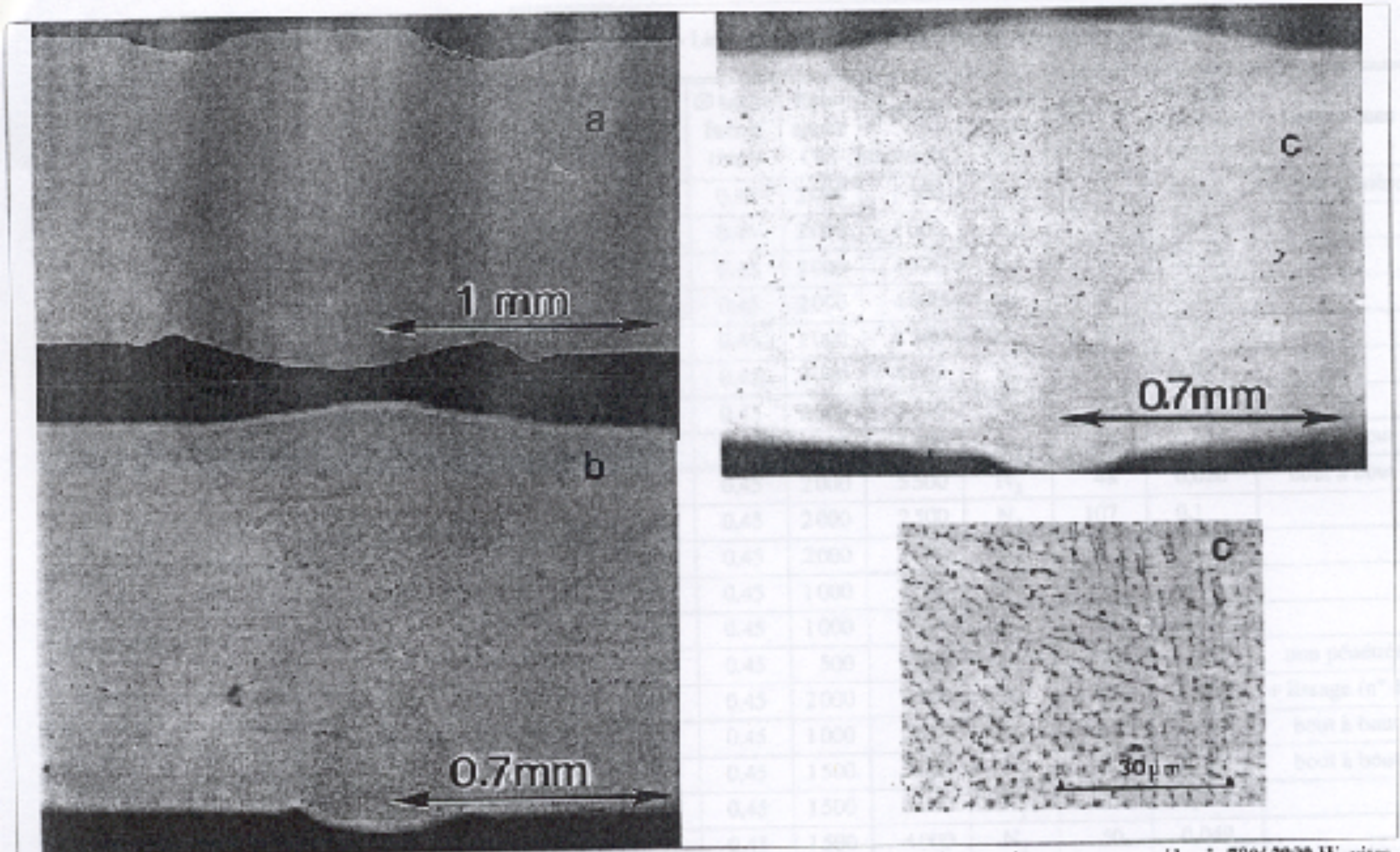

Fig. 5 - Aspect général du cordon fondu de l'acier UNS 21904 : a) laser pulsé (200 Hz, durée de pulse 1,2 ms, puissance moyenne/de pic 700/ 2900 W, vitesse 0,45 m/min) : légère surpénétration avec deux caniveaux en couronne ; b) laser continu (essai n°21, annexe I) ; c) laser continu (essai n°15 - annexe I) zone ferritique, détail.

S. SGOBBA, C. BOUDOT, Soudabilité laser d'aciers inoxydables austénitiques, Matériaux et Techniques **95**, n°11-12, p. 23 (1997).

LHC beam screen

Steels	C	Mn	Ni	Cr	Mo	Si	N	P	S	B
P506	0.012	12.05	10.90	19.18	0.86	0.23	0.33	0.005	0.001	<0.001

a

b1

500 µm

1 mm

c

b2

Base metal

Weld metal

250 µm

1 mm

S. Sgobba, G. Hochörtler, A New Non-Magnetic Stainless Steel for Very Low Temperature Applications, Proceedings of the International Congress Stainless Steel 1999: Science and Market, Chia Laguna (I), 6-9 June 1999, Vol. 2, p. 391-401

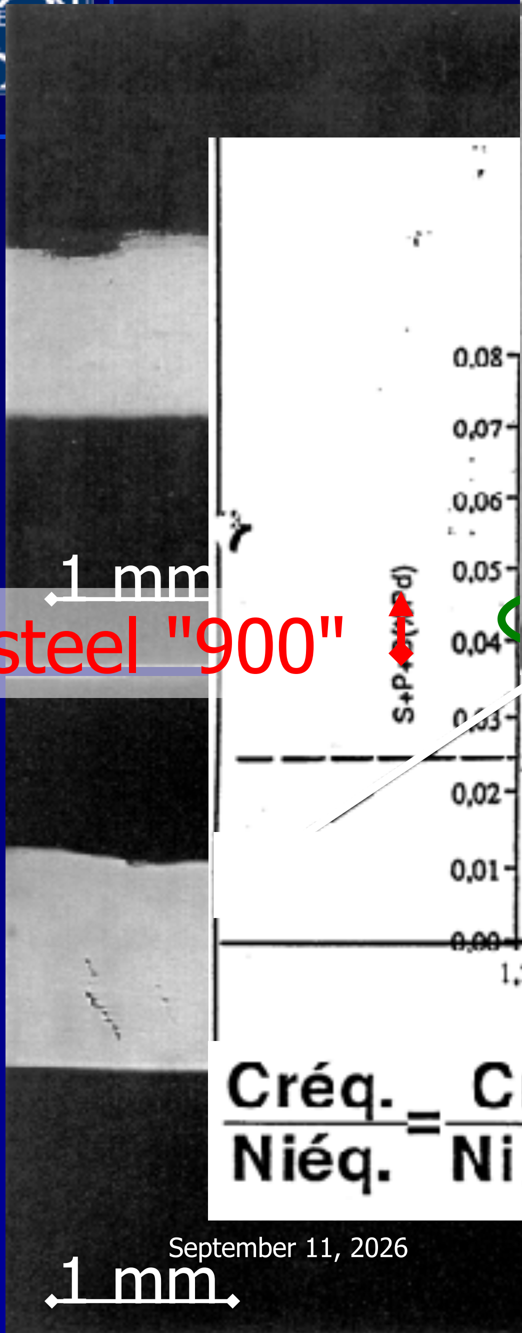

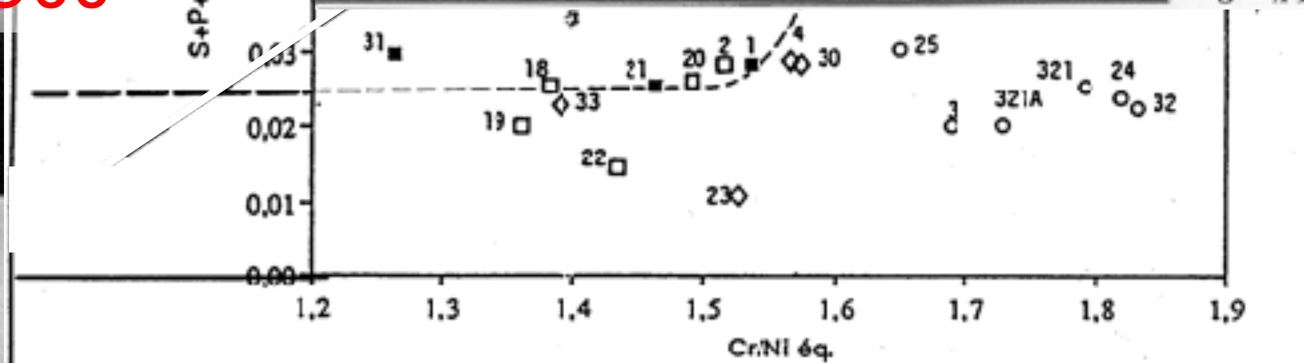

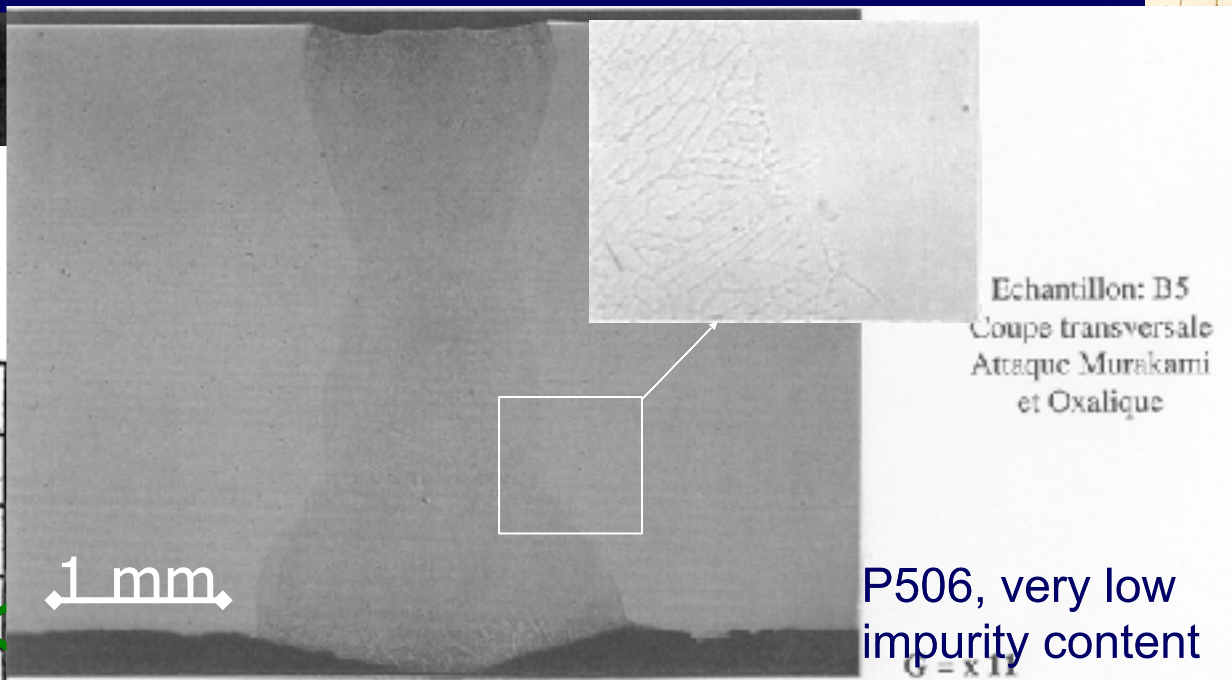

$$\frac{\text{Créq.}}{\text{Niéq.}} = \frac{Cr + 1{,}37Mo + 1{,}5Si + 2Nb + 3Ti}{Ni + 0{,}31Mn + 22C + 14{,}2\ldots}$$

S. Sgobba: proc. Cycle Métaux et Procédés, CIP - Tramelan /CH, 1996, p. 8/1-10 and EST/SM-MB report n° 96/10/16

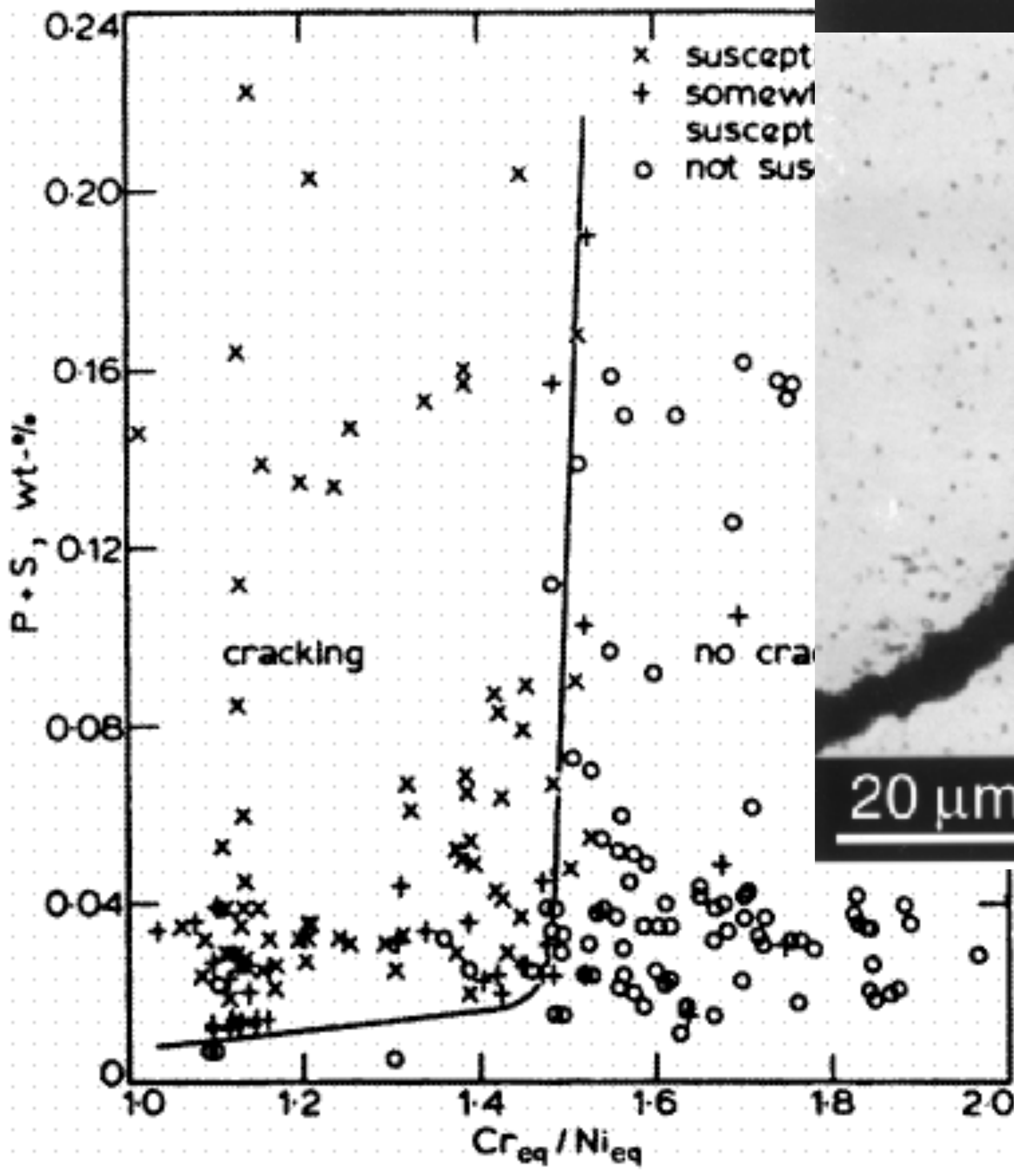

Figure 2. Cracking susceptibility of 300 series stainless steel based on Cr-Ni equivalence from Hammar and Svenson, ref. 13.

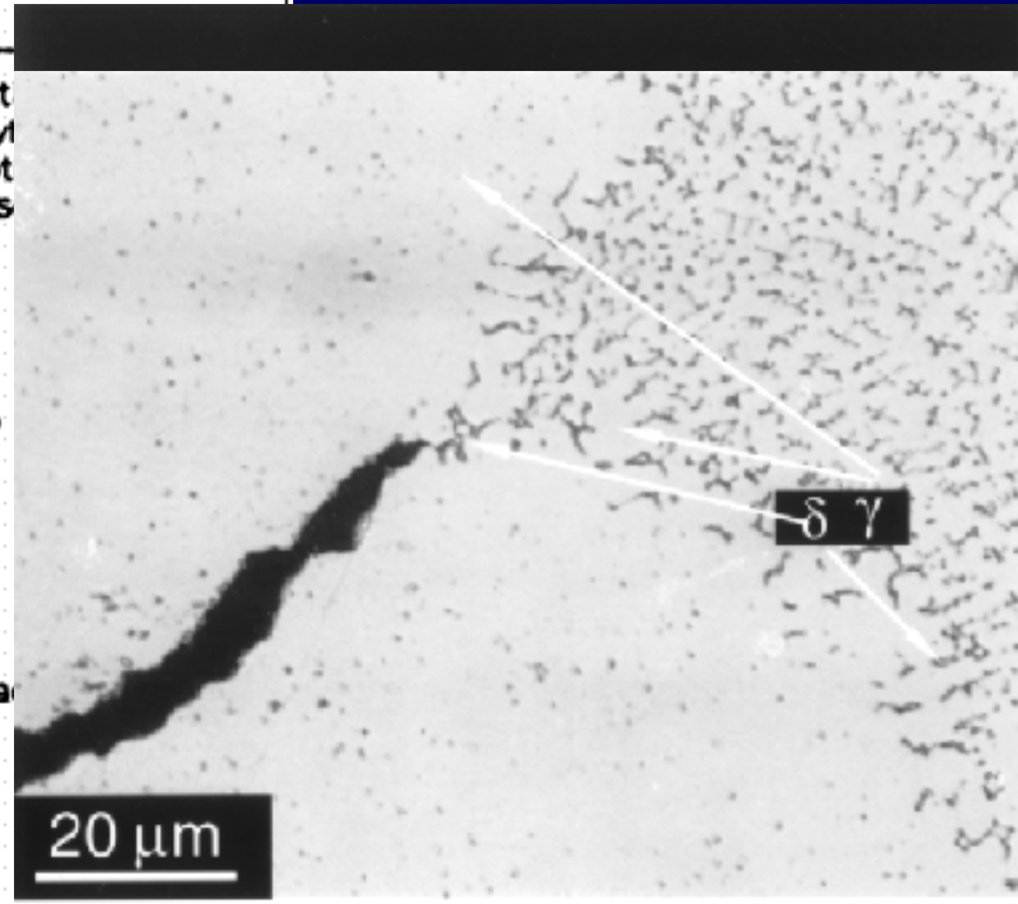

LHC beam screen: stainless steels, specific features at cryogenic T

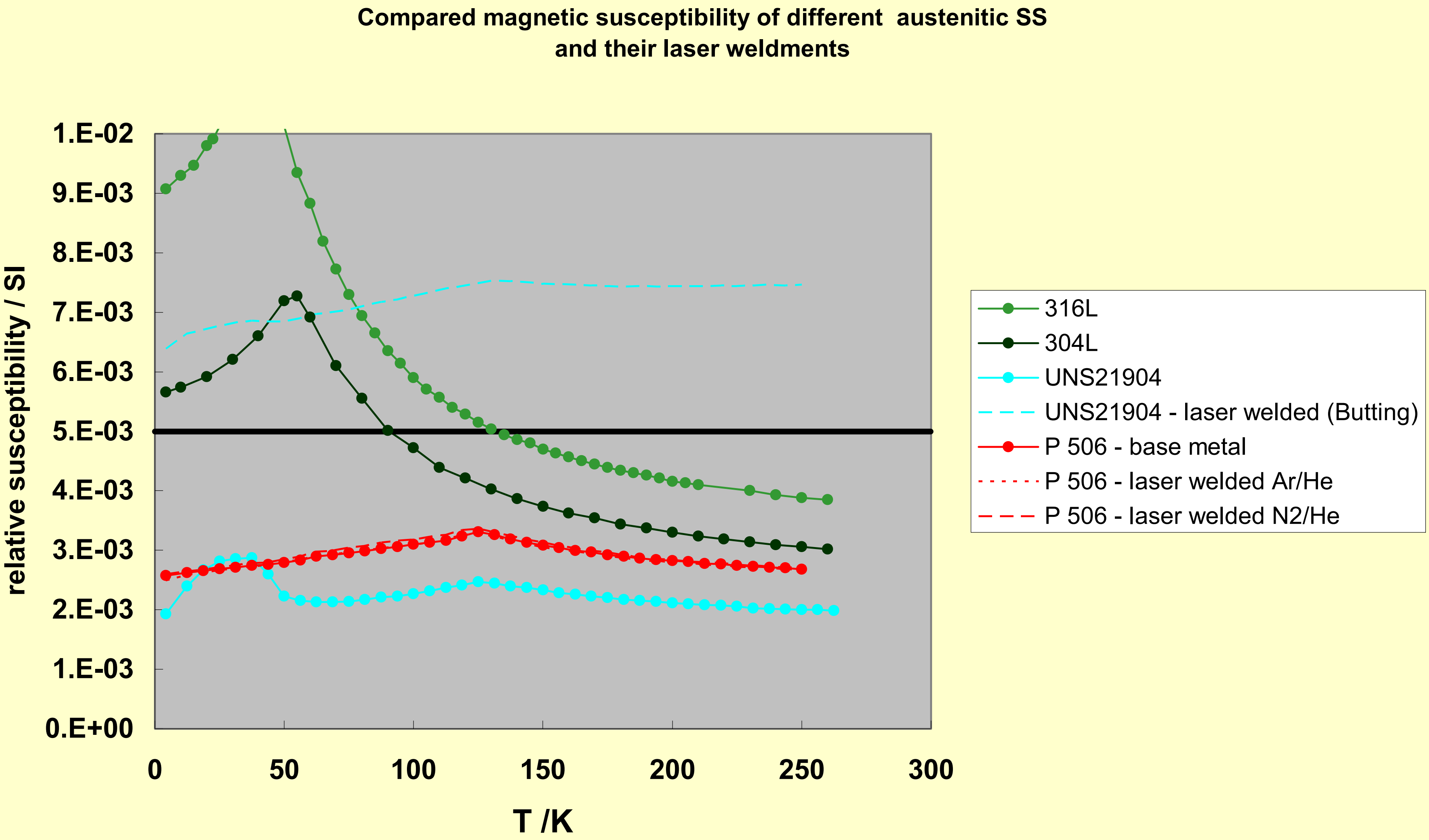

S. SGOBBA and G. HOCHOERTLER : A New Non-Magnetic Stainless Steel for Very Low Temperature Applications, Proceedings of the International Congress Stainless Steel 1999: Science and Market, Chia Laguna /IT, 6-9 June 1999, Vol. **2**, p. 391-401

LHC beam screen: stainless steels, specific features at cryogenic T

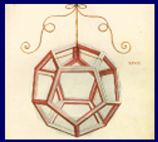

Warnes law:

$$T_{af}(K) = 90 - 1.25Cr - 2.75Ni - 5.5Mo - 14Si + 7.75Mn$$

P506, predicted T_{af} = 121.5 K, measured 125.7 K

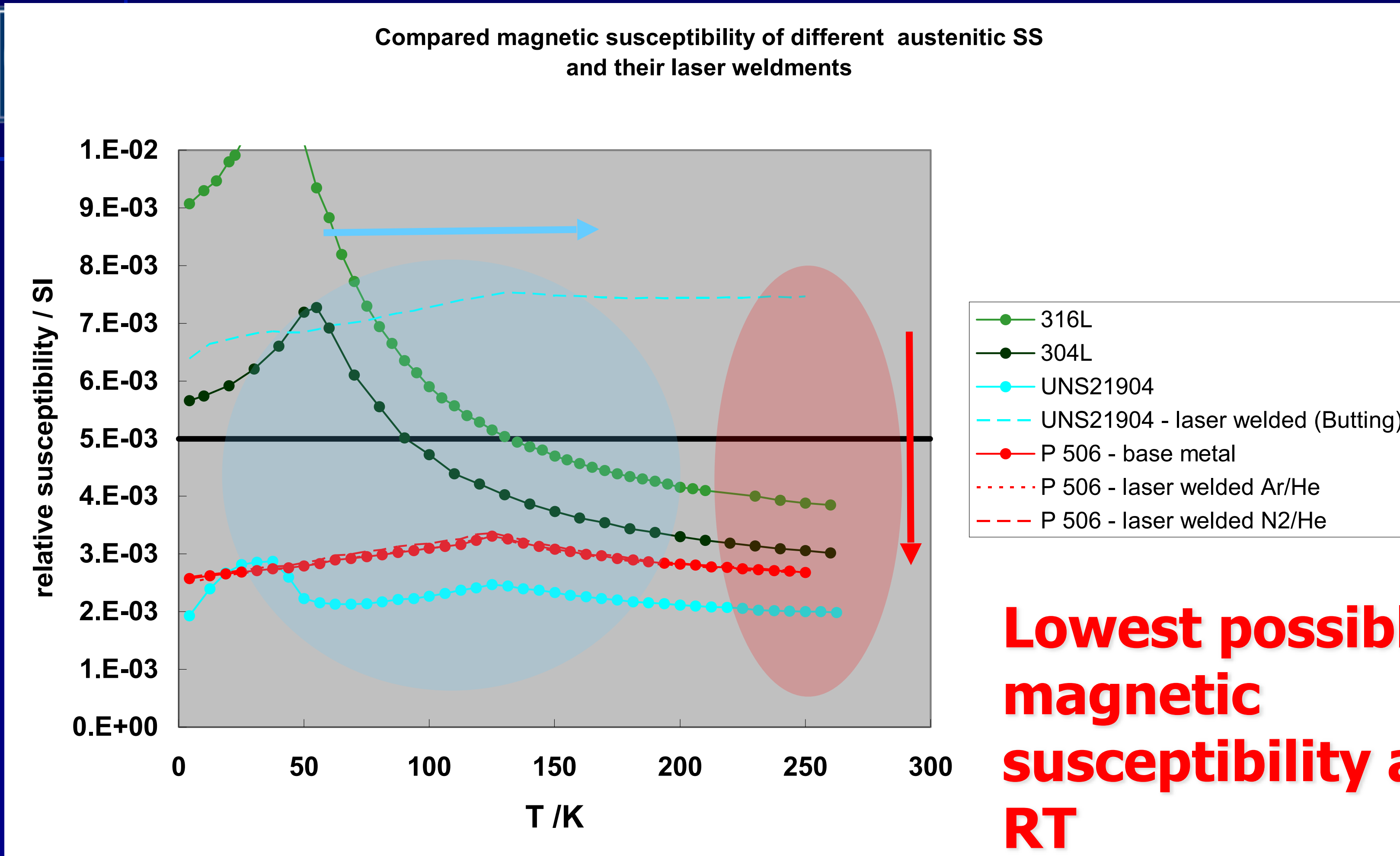

Lowest possible magnetic susceptibility at RT

Highest possible temperature of antiferromagnetic transition

LHC beam screen: stainless steels, specific features at cryogenic T

$$T_{af}(K) = 90 - 1.25Cr - 2$$

Highly non-magnetic sta
N) steels

Specially true for very lo

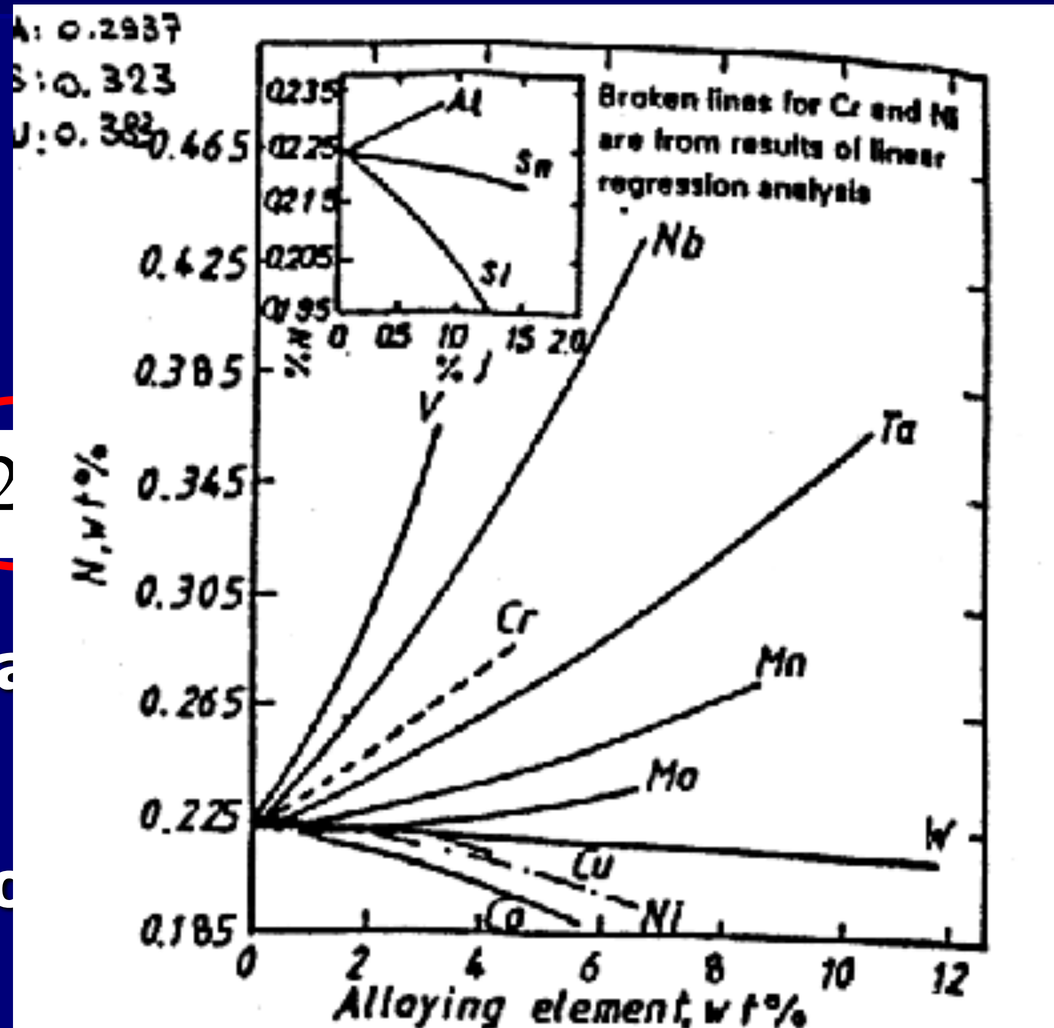

Fig. 3—Effect of alloying elements on the solubility of nitrogen in liquid Fe-18%Cr-8%Ni alloys at 1600°C and 1 atm N_2[3]

LHC beam screen: stainless steels, specific features at

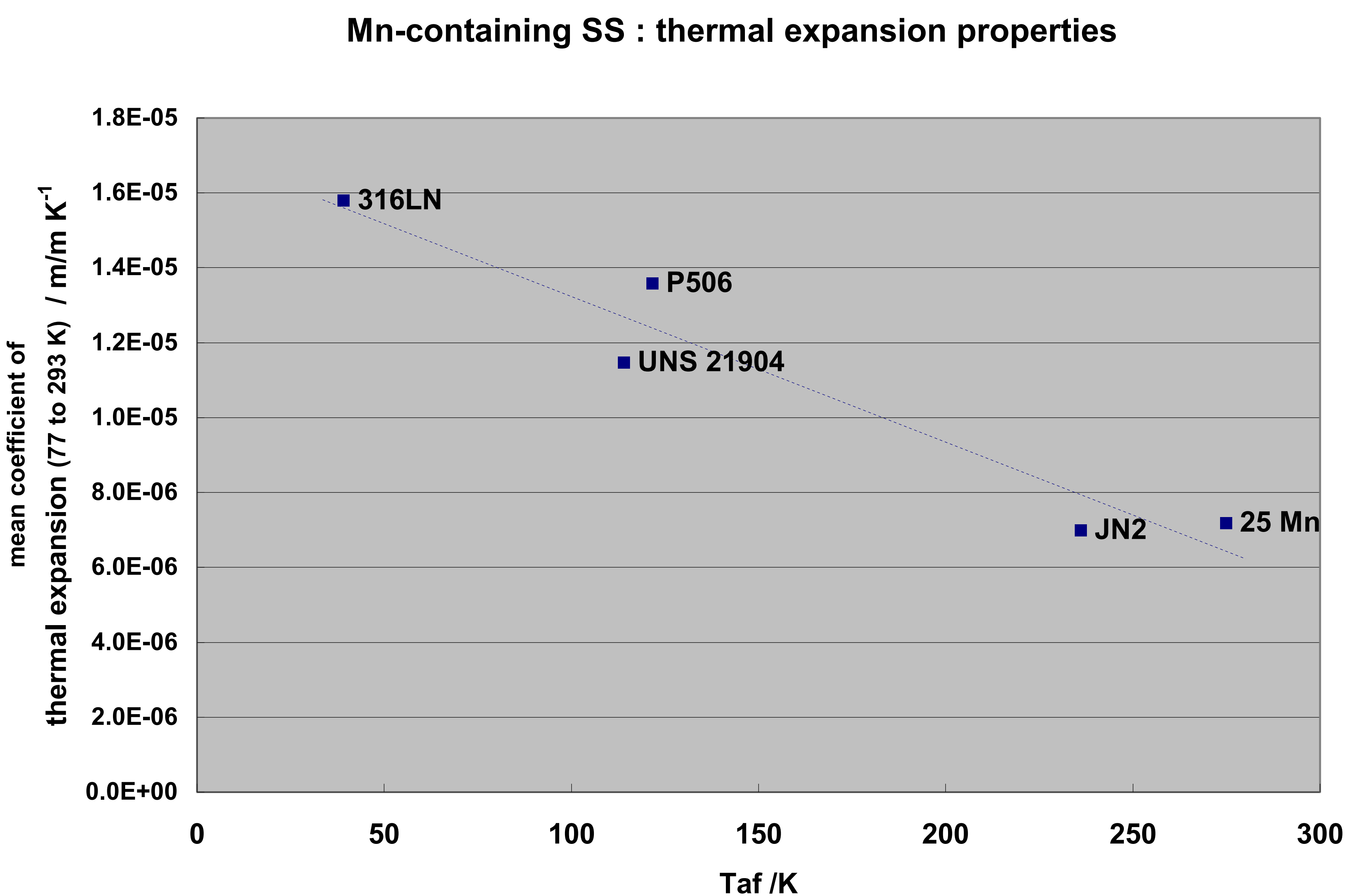

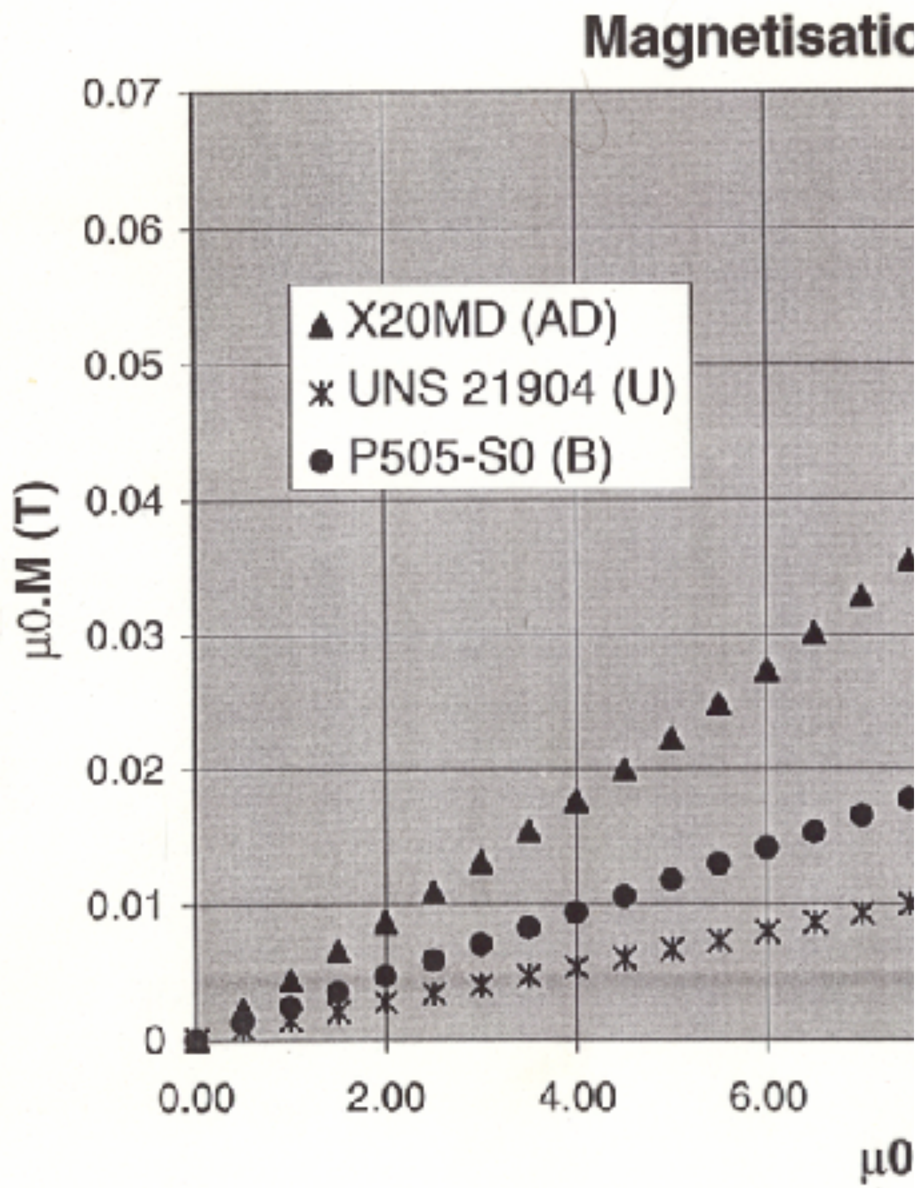

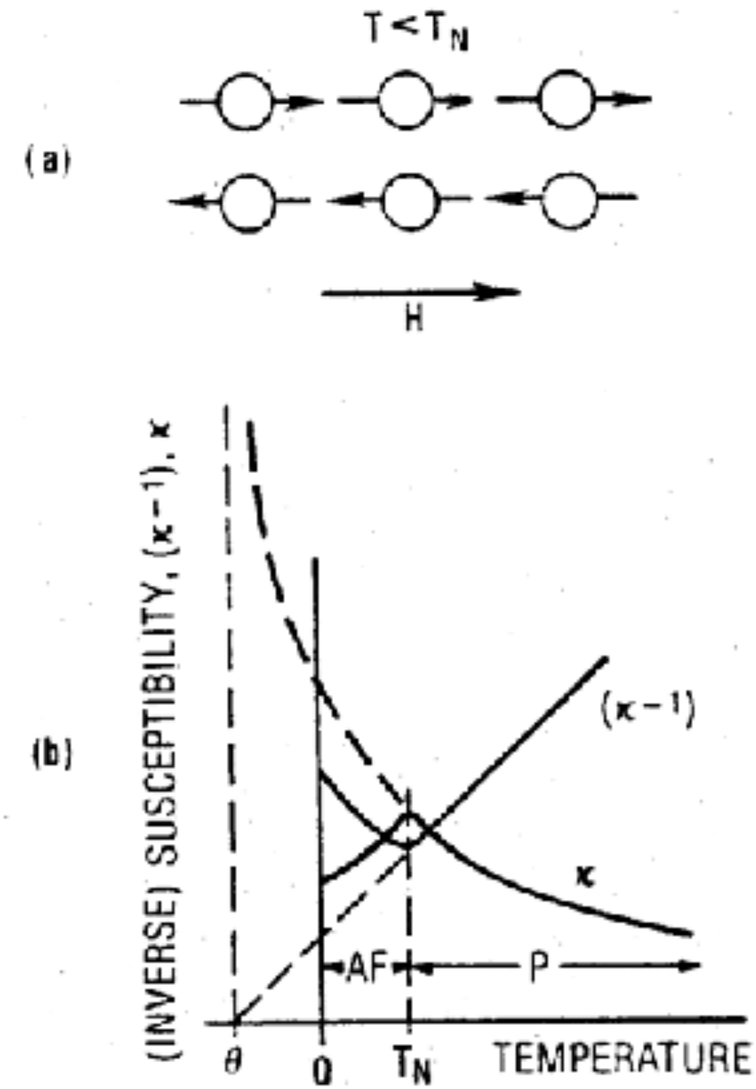

Figure 6.8 (a) Antiferromagnetic alignment of atomic magnetic moments. (b) Susceptibility and reciprocal susceptibility vs. temperature showing antiferromagnetic (AF) and paramagnetic (P) intervals.

Phase transformationd and their influence on magnetic behaviour

Steels	C	Mn	Ni	Cr	Mo	Si	N	P	S	B
P506	0.012	**12.05**	10.90	19.18	0.86	0.23	**0.33**	0.005	0.001	<0.001
YUS130S	0.09	**10.70**	6.60	18.00	0.10	0.40	**0.32**	0.022	0.004	-
KHMN30L	0.10	**28.00**	0.82	6.70	-	0.60	**0.10**	0.022	0.004	-
316 LN	*0.021*	***1.26***	*13.03*	*17.33*	*2.61*	*0.61*	***0.16***	*0.025*	*0.0008*	*0.0011*

Table 1: Chemical composition (% in weight) of the three austenitic steels. For comparison, the typical composition of standard AISI 316 LN stainless steel is given.

Table 4 shows the values of the temperature Md30, calculated for the three Mn steels and 316 LN according to the relationship of Nohara et al. (11):

$$Md30\ (^{o}C) = 551 - 462(C+N) - 9.2Si - 8.2Mn - 13.7Cr - 29(Ni+Cu) - 68Nb - 1.42(8-\nu) \qquad (2)$$

where ν is ASTM grain size number.

Steel	P506	YUS130S	KHMN30L	*316 LN*
Md30 (^{o}C)	-291	-171	105	*-167*

Table 4: Calculated Md30 of the three high Mn steels. For comparison, value of 316 LN is calculated.

Phase transformationd and their influence on magnetic behaviour

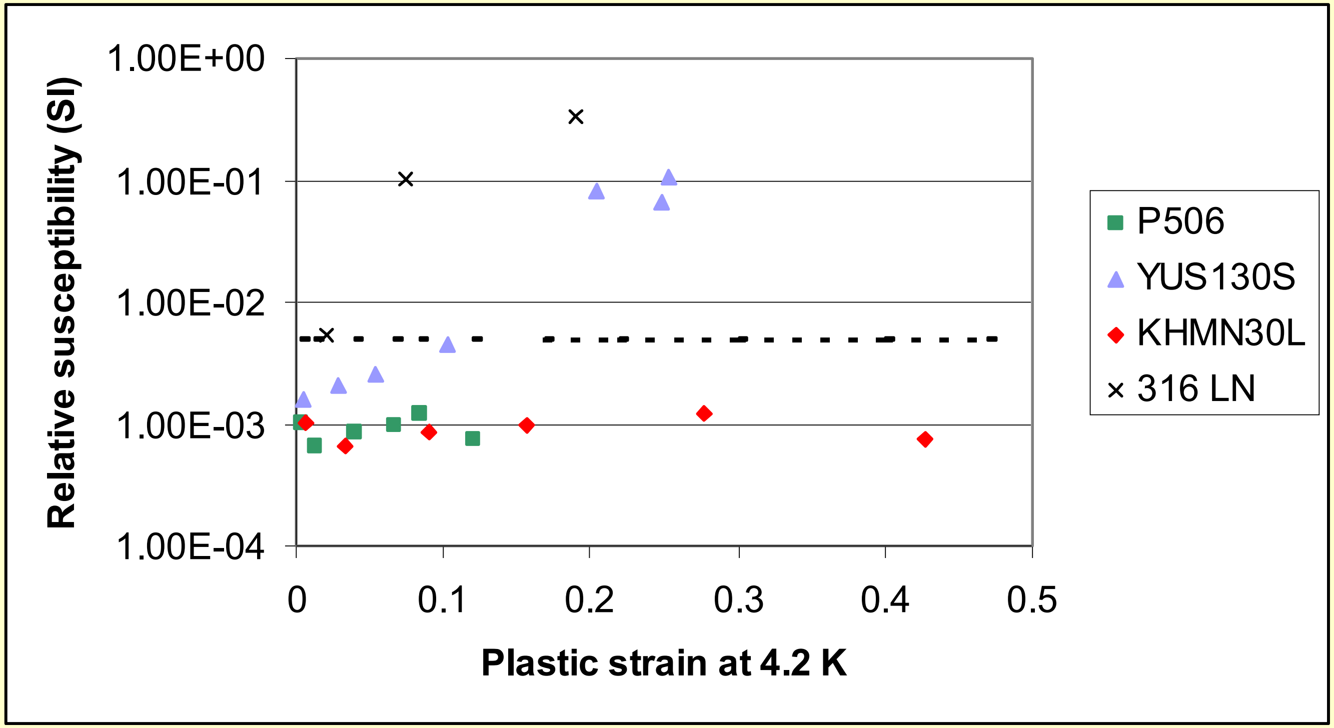

Figure 2: Evolution of room temperature relative magnetic susceptibility with plastic strain at 4.2 K. Values are average values on three tests performed for each plastic strain level. For comparison, values for standard 316 LN stainless steel are also given. The dashed line corresponds to a value of $\chi_r = 5 \cdot 10^{-3}$.

K. COUTURIER, S. SGOBBA, Phase Stability of High Manganese Austenitic Steels for Cryogenic Applications, Proceedings of the "Materials Week" European Conference, Munich, Germany, September 25-28, 2000,

http://www.proceedings.materialsweek.org/proceed/mw2000_432.pdf

Phase transformationd and their influence on magnetic behaviour

Start of strain induced martensitic transformation = change of curvature

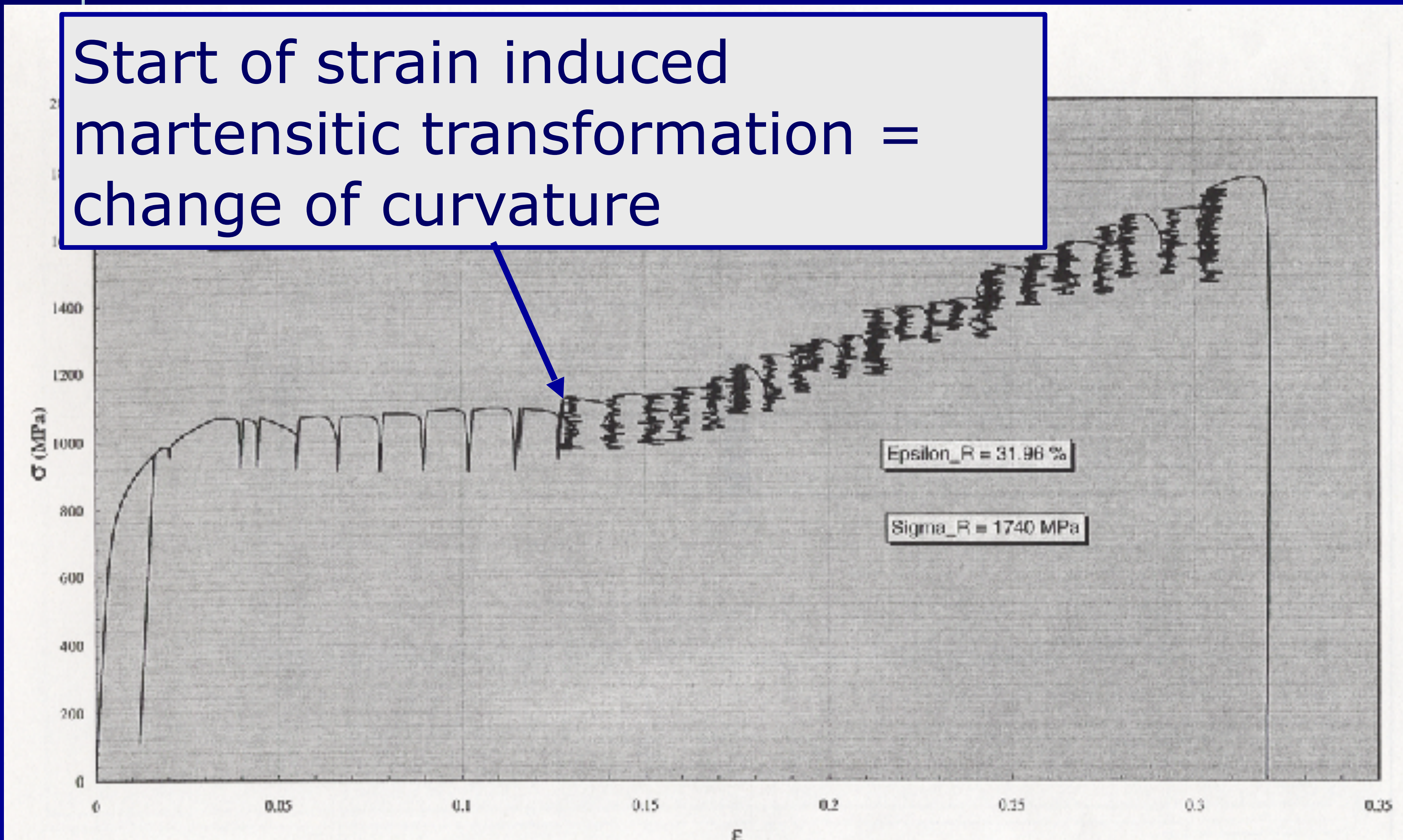

Phase transformationd and their influence on magnetic behaviour

Element	Specification (CERN requirement)	Thickness 0.15 mm content %	Thickness 0.25 mm content %
C	0.030 max.	0.027	0.024
Si	1.00 max.	0.598	0.492
Mn	2.00 max.	1.557	0.872
P	0.030 max.	0.022	0.025
S	0.010 max.	0.0009	0.0022
Cr	16.00 - 18.50	17.99	17.91
Ni	11.00 - 14.00	10.99	11.03
Mo	2.00 - 2.50	2.032	1.97
Co	0.20 max.	0.122	0.195
N	0.050 max.	0.0375	0.0274

Table 1 Results of chemical analysis for fine gauge 316L plates, thickness 0.15 and 0.25 mm.

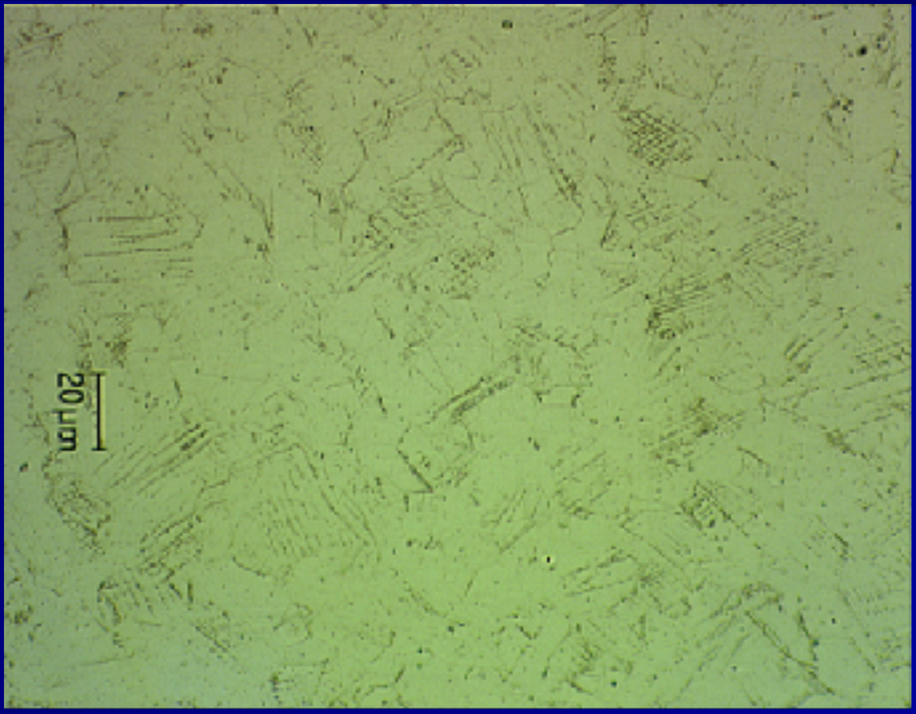

Partially transfor… …ained 6.5% at 4.2 K. Martensite is con… …g during tensile deformation at 4… …n Fig. b (C. GARION, S. SGOBBA, B. SKO… …ion in 316L stainless steel at cryogenic tem… Submitted for publication in International J…

Thickness [mm]	Ms [K]	Md30 [K]
0.15	< 0	265
0.25	< 0	266

Table 2 Temperatures Ms and Md30 estimated for two different 316L heats

Phase transformationd and their influence on magnetic behaviour

P506, tensile stress-strain curves

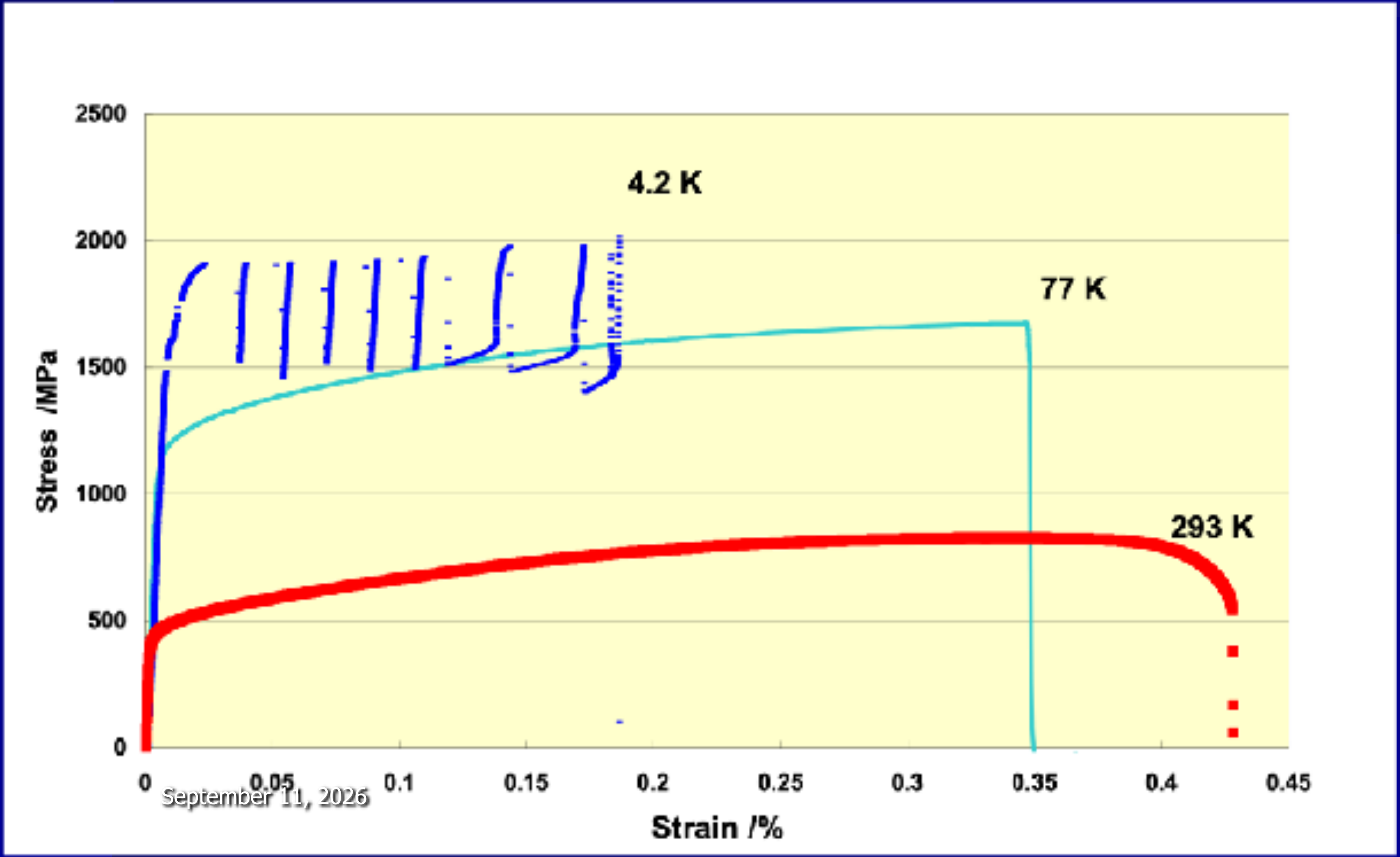

Structure and contents

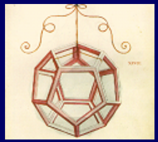

(I) Magnetic properties of materials: types of magnetic behaviour

(II) Conventional and innovative magnetic materials of interest for accelerator technology

(III) Methods of measurements

Magnetic lag

Innovative material solutions for magnets

(IV)	(a)	"Non-magnetic" materials, phase stability and phase transformations: LHC beam screen
	(b)	Powder metallurgy applied to structural materials: end covers of LHC dipole magnets

LHC DIPOLE : STANDARD CROSS-SECTION

CERN AC/DI/MM - HE107 - 30 04 1999

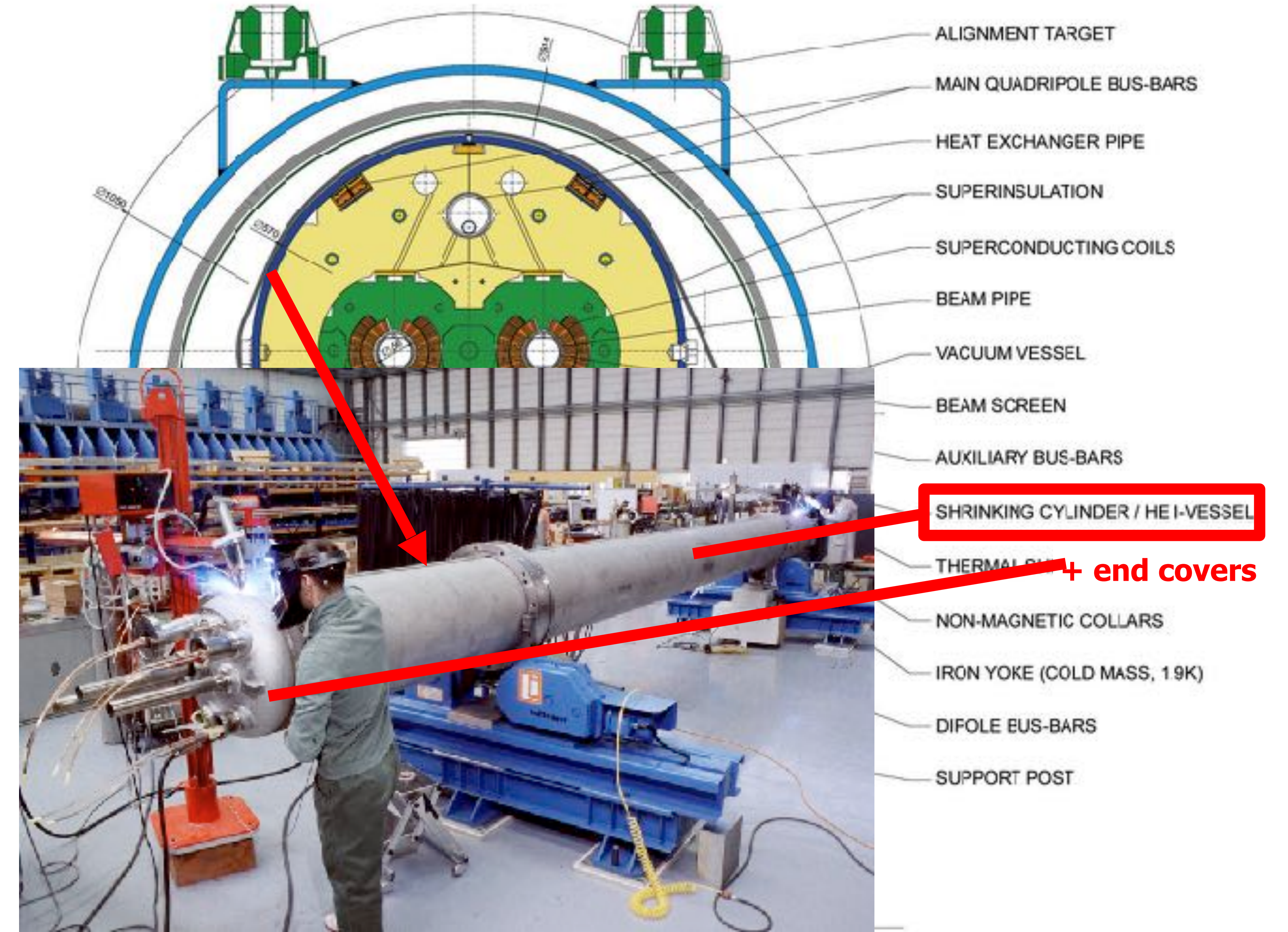

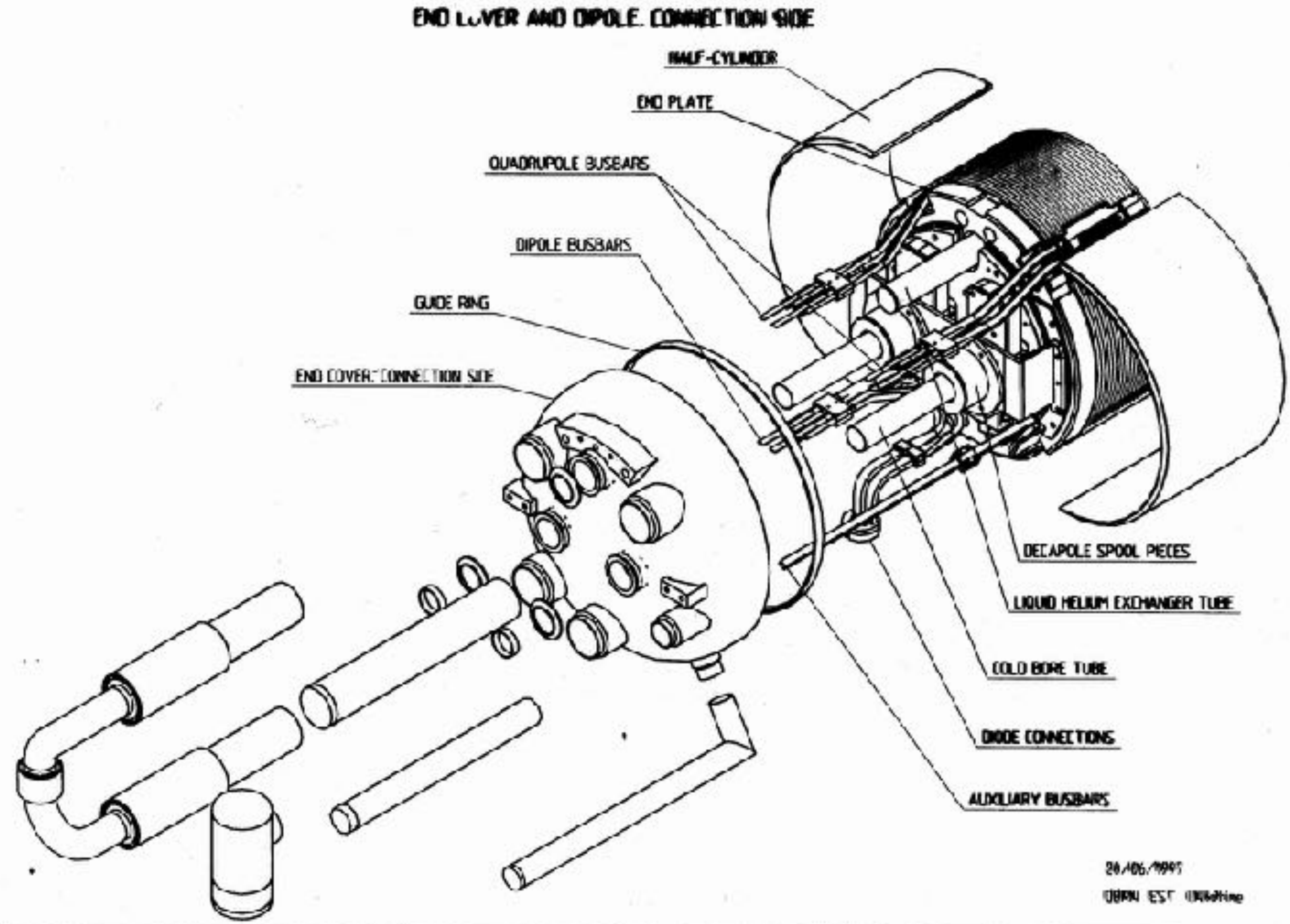
END COVER AND DIPOLE CONNECTION SIDE
HALF-CYLINDER
END PLATE
QUADRUPOLE BUSBARS
DIPOLE BUSBARS
GUIDE RING
END COVER: CONNECTION SIDE
DECAPOLE SPOOL PIECES
LIQUID HELIUM EXCHANGER TUBE
COLD BORE TUBE
DIODE CONNECTIONS
AUXILIARY BUSBARS

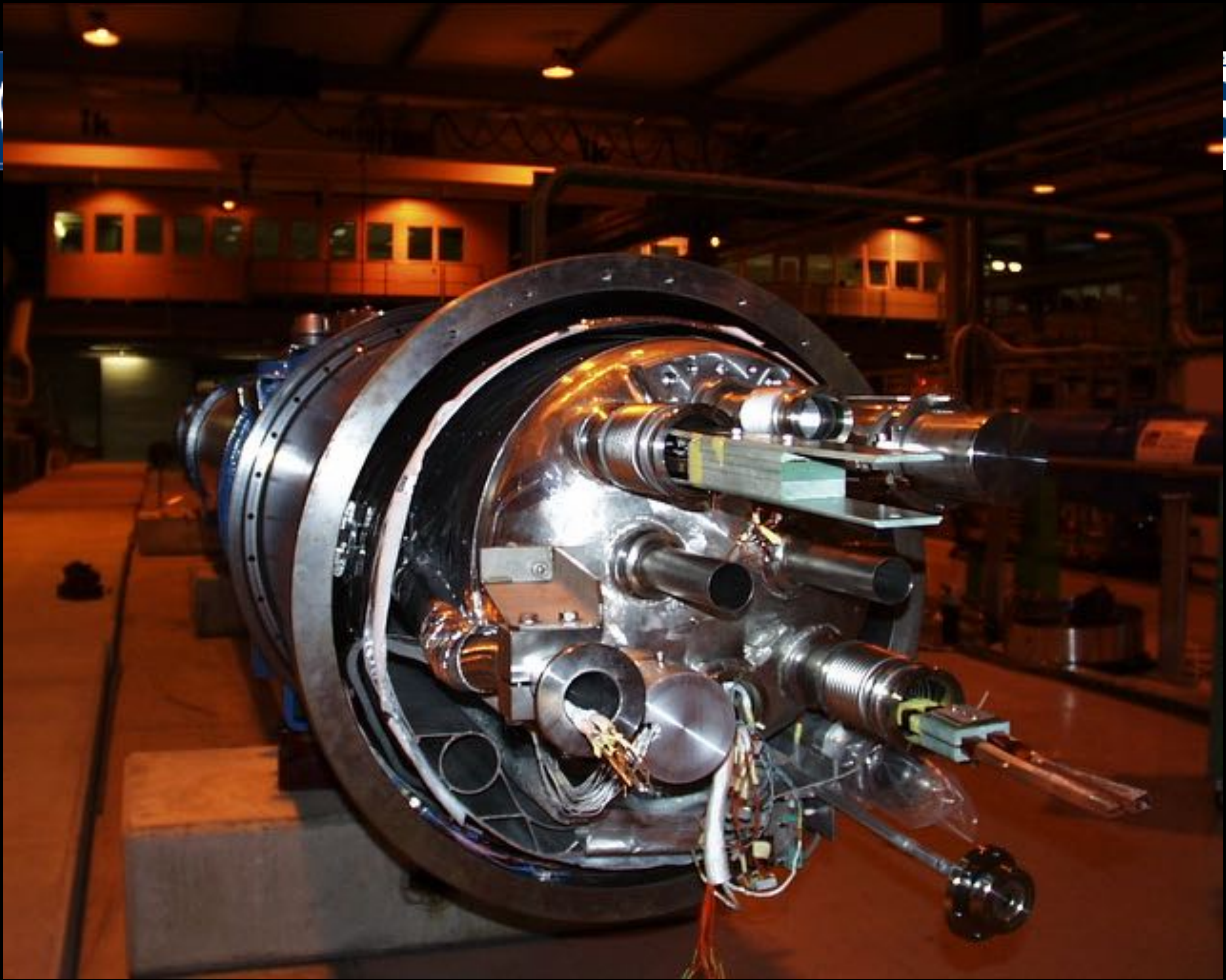

Dimensions and working conditions

- **depth : 194 mm**
- **diameter : 580 mm**
- **wall thickness : 12 mm**
- **weight : approx. 50 kg**

- **leak tight to gazeous He at 300 K under 2.6 MPa *(test pressure)***
- **leak tight to superfluid He at 1.9 K under 0.13 MPa *(operating pressure)***
- **25 thermal cycles 1.9 K ⇒ 300 K ⇒ 1.9 K *(over 20 years)***

PM 316LN, circular MIG weld

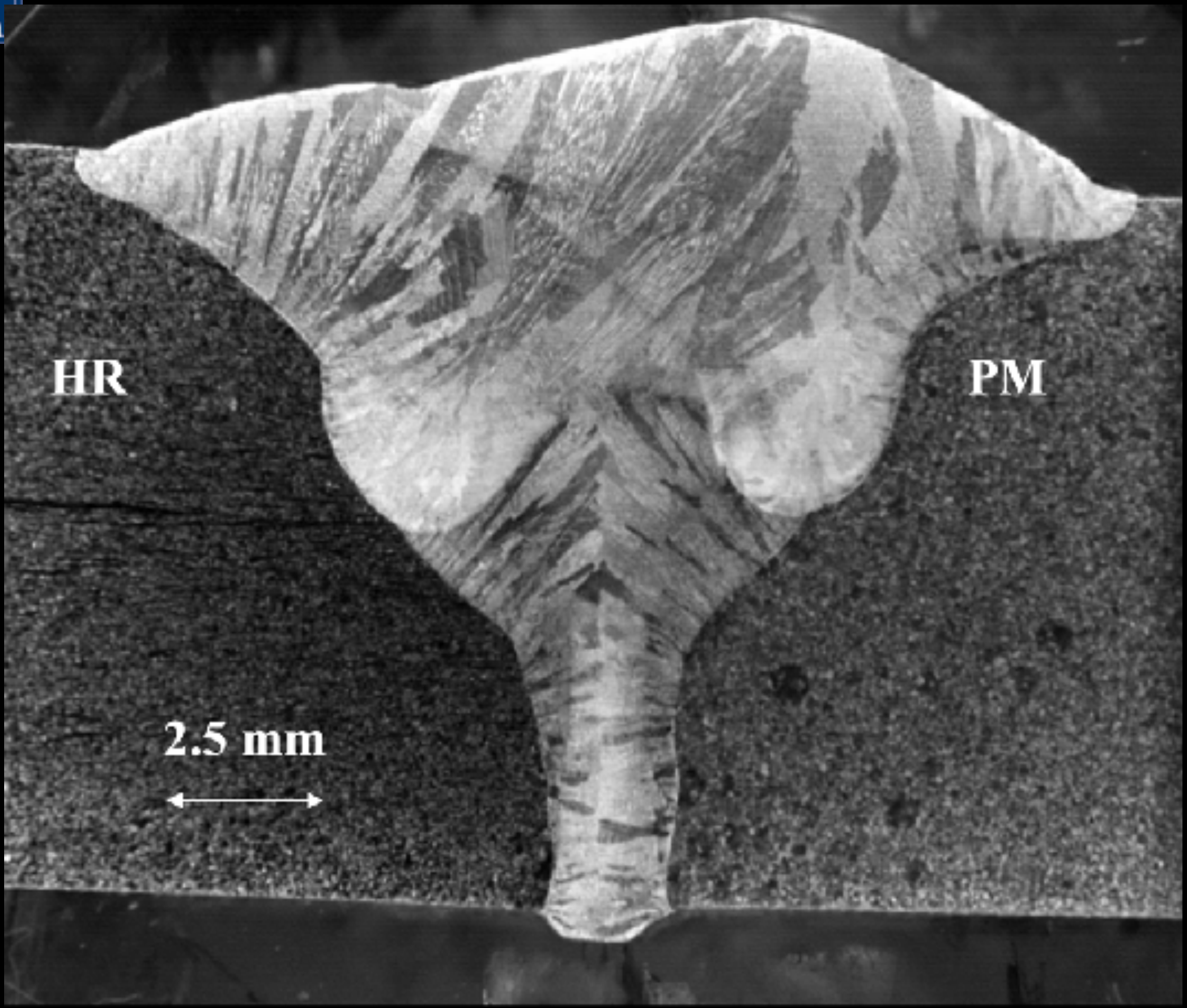

316LN, orbital TIG weld

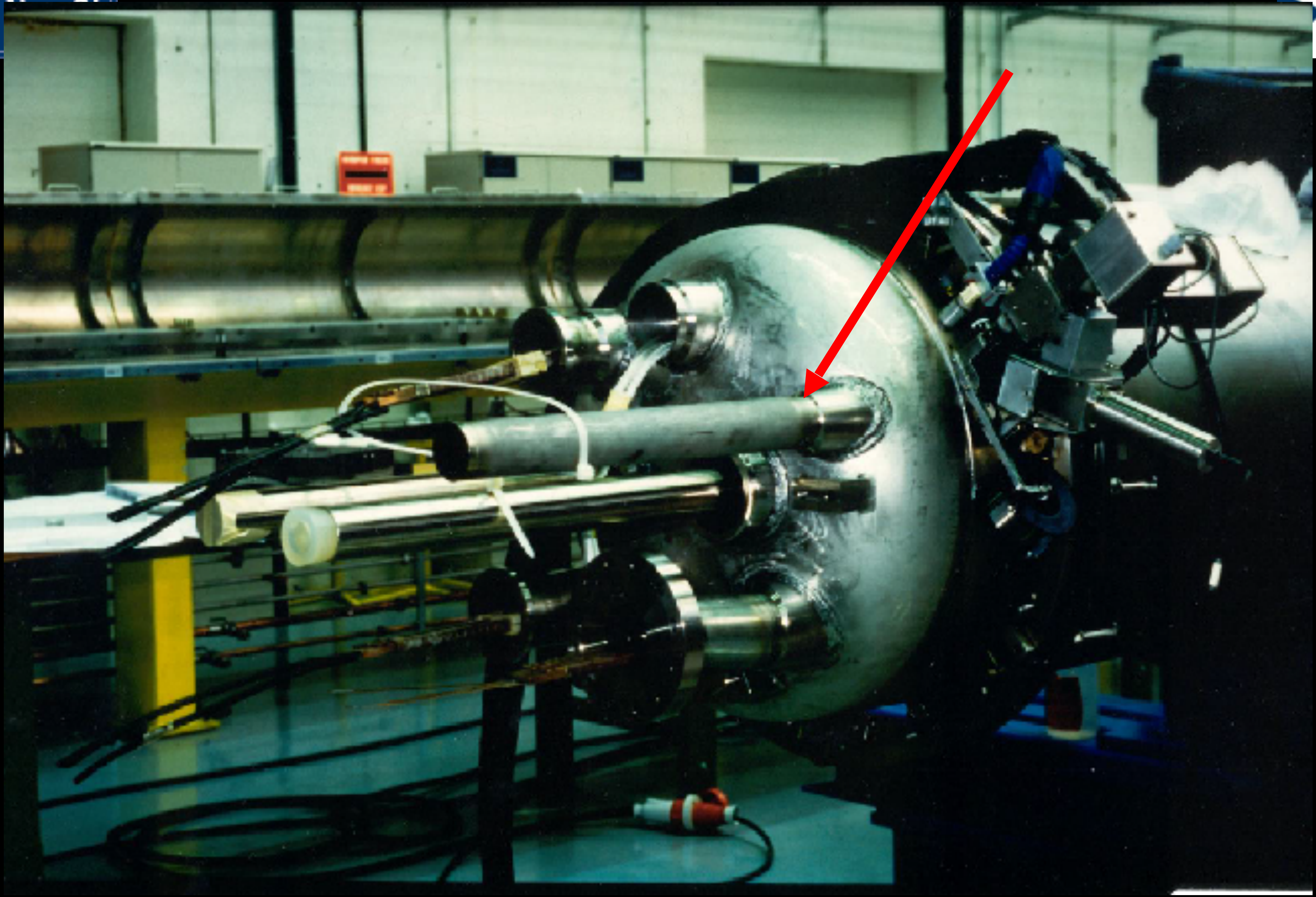

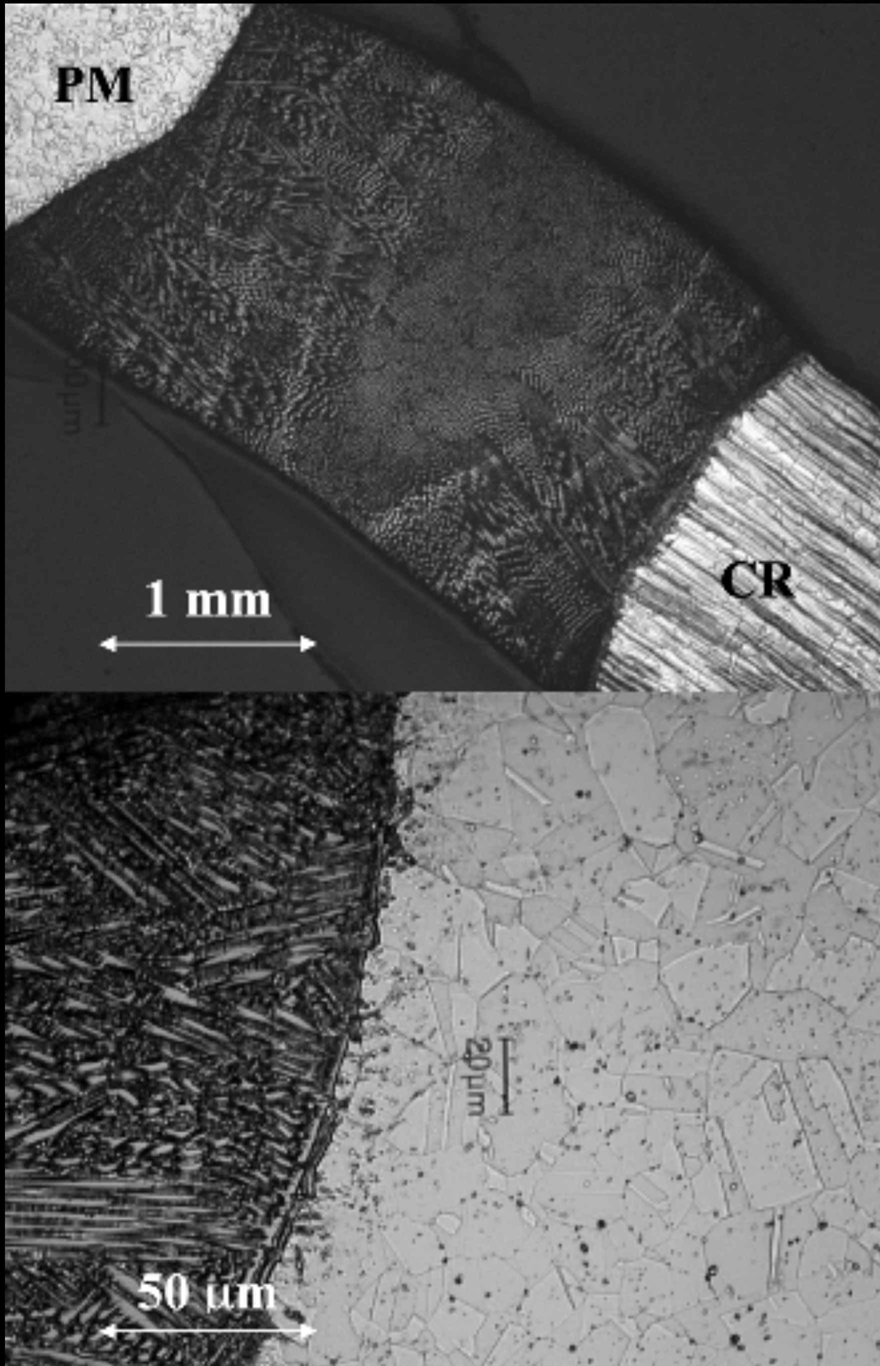

PM 316LN, orbital TIG weld

Welding details :

Travel speed:	1.5E-02m/s	Arc length:	1.5E-03m
Peak current:	68 A	Tip angle	45°
Base current:	32 A	Gas flux and flow rate:	
Peak time:	0.2 s	Shielding:	Ar, 1/6 l/s
Base time:	0.2 s	Backing:	Ar, 1/12 l/s

McHenry H.I., The Properties of Austenitic Steels at Cryogenic Temperature

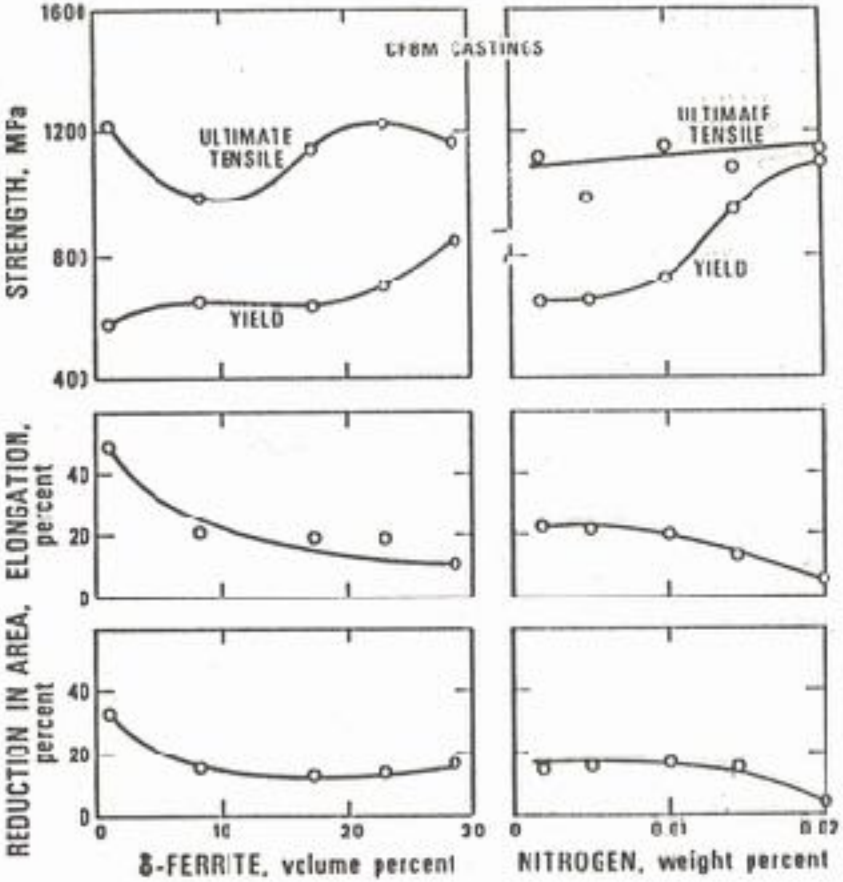

Fig. 18. The effect of δ-ferrite and nitrogen content on the tensile properties at 4 K of CF8M austenitic stainless steel castings. The castings in the δ-ferrite study contained 0.05% N and the castings in the nitrogen study contained 9 ±1% δ-ferrite.[31]

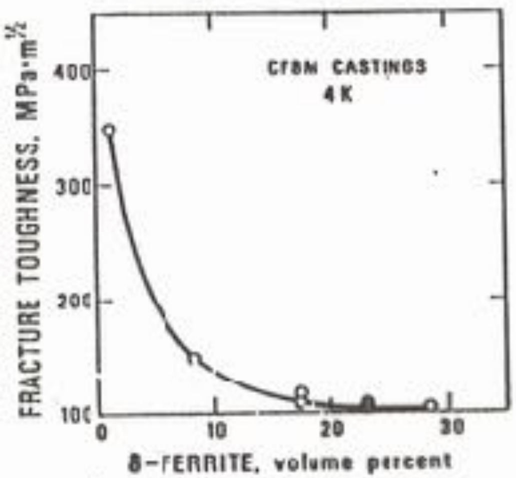

Fig. 19. The effect of δ-ferrite on the 4-K fracture toughness of CF8M austenitic stainless steel castings containing 0.05% N.[31]

H. I. McHENRY

HIPed AISI 316LN end covers for CERN LHC project (courtesy of Metso)

Main manufacturing stages

- inert gas atomization of AISI 316LN powder
- capsule manufacture
- powder filling, evacuation and sealing
- hot isostatic pressing (1180 °C, 100 MPa, 4 h)
- can removal by pickling
- heat treatment (1060 °C, 2 h, water quenching)
- machining
- NDT by 100 % ultrasonic and liquid penetrant inspection

Hot Isostatic Pressing

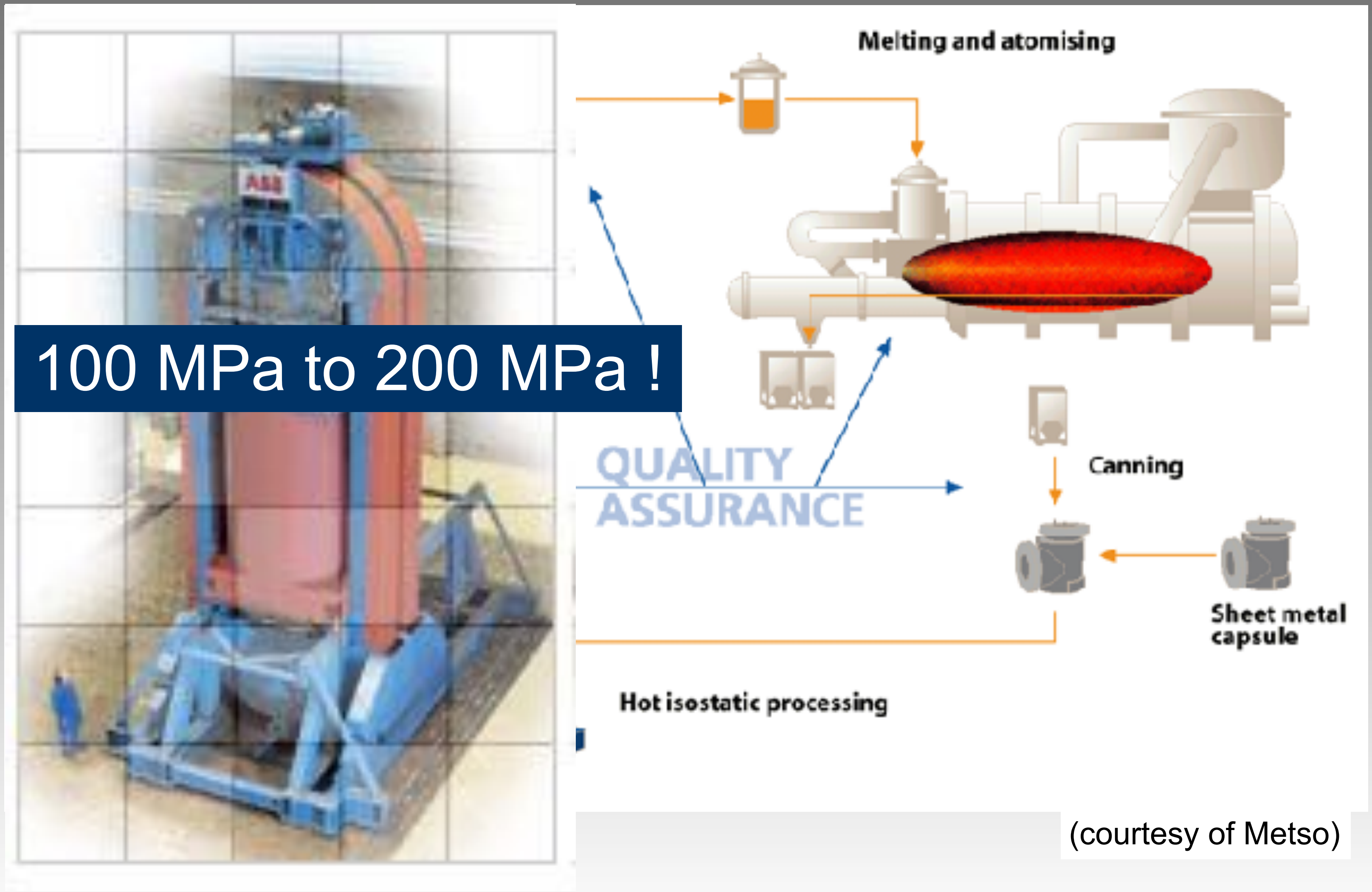

(courtesy of Metso)

HIPed AISI 316LN end covers for CERN LHC project (courtesy of Metso)

Liquid penetrant inspection

Microstructu rougth

100 μm

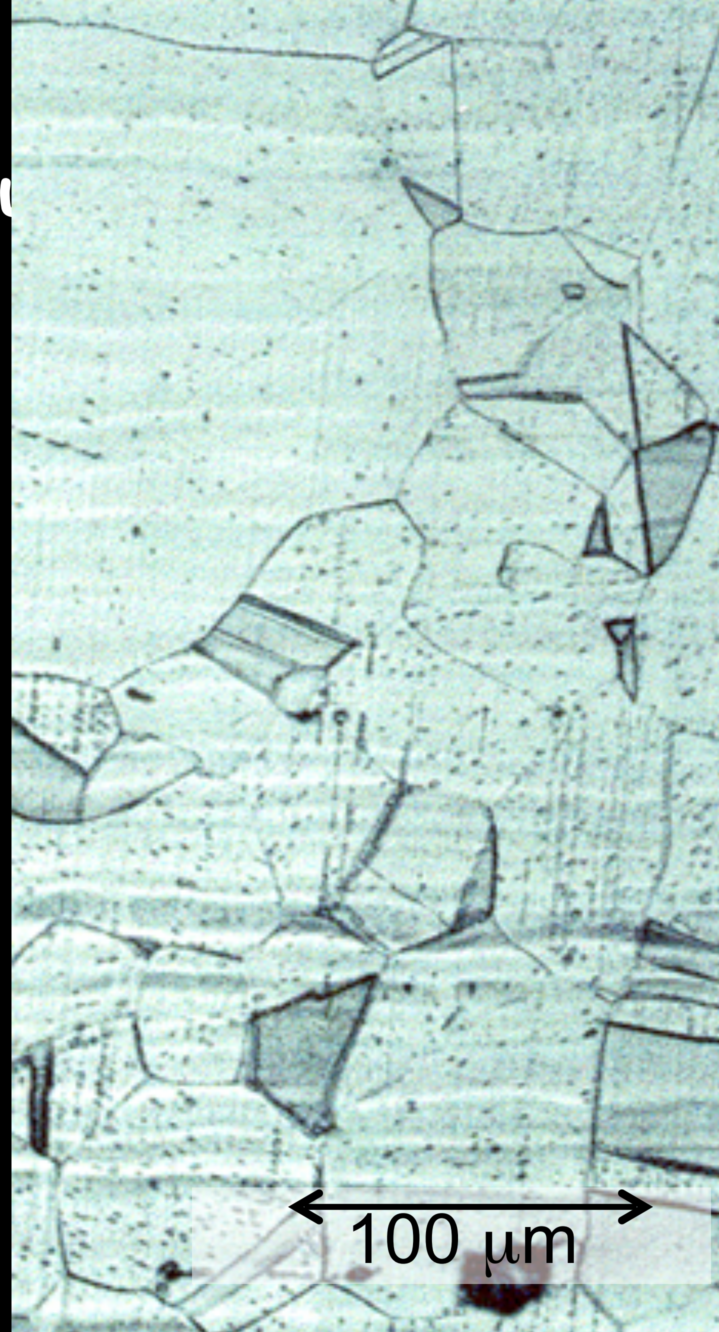

Microstructure, comparison 2: cast

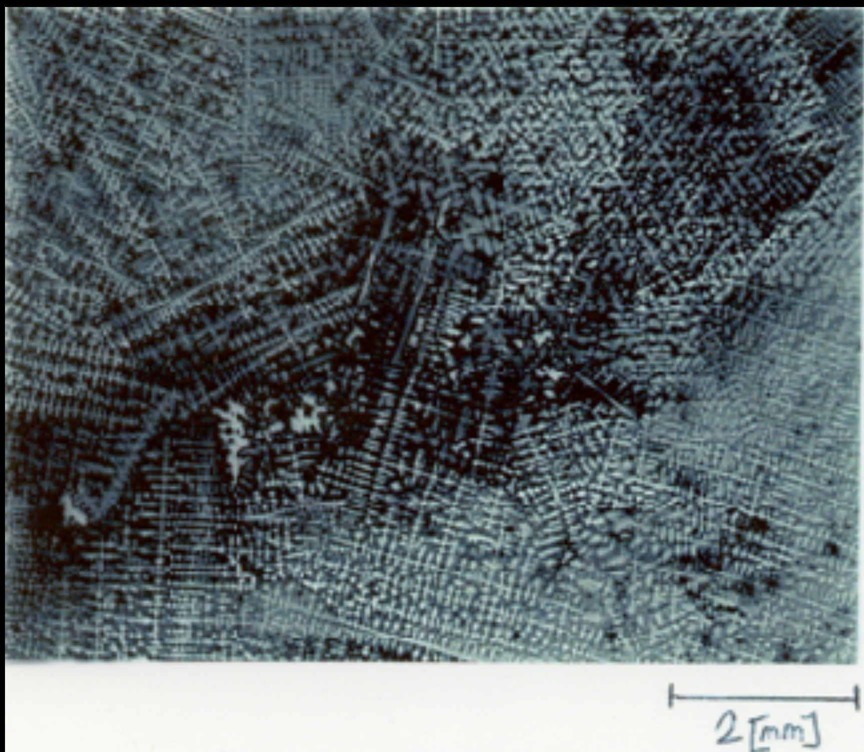

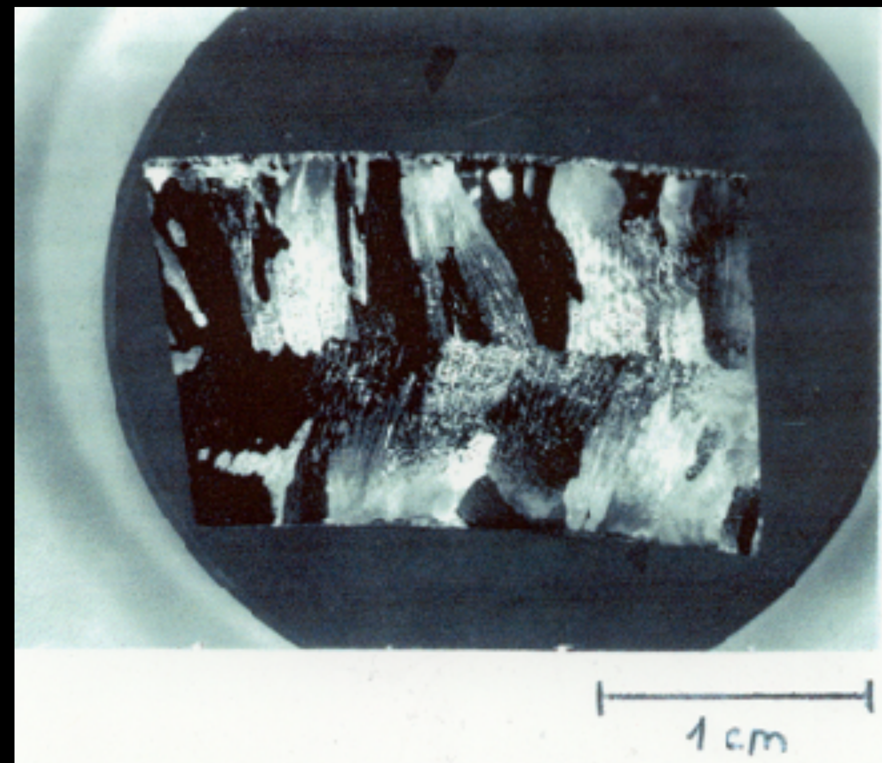

Thermal contraction

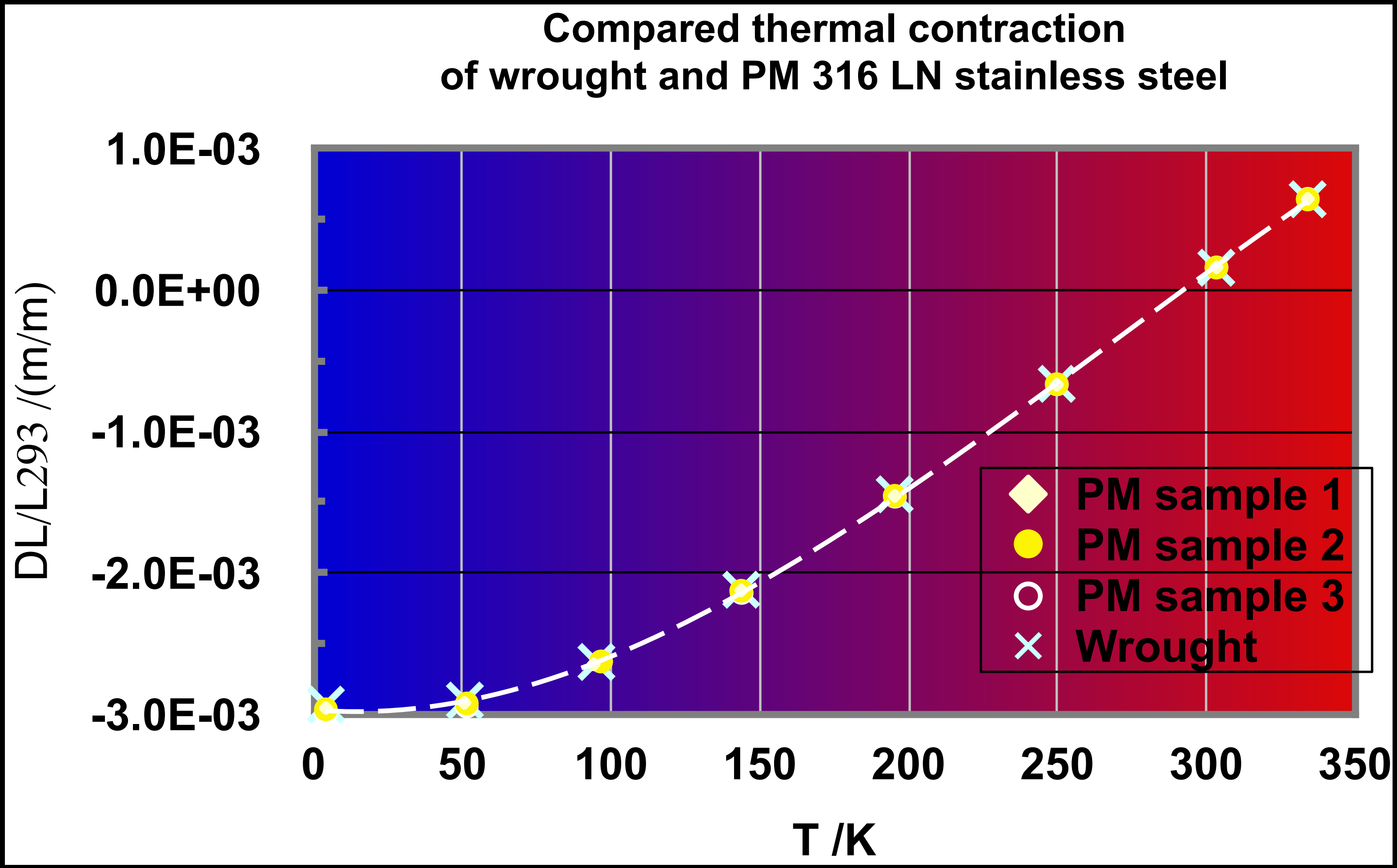

Mechanical properties: tensile

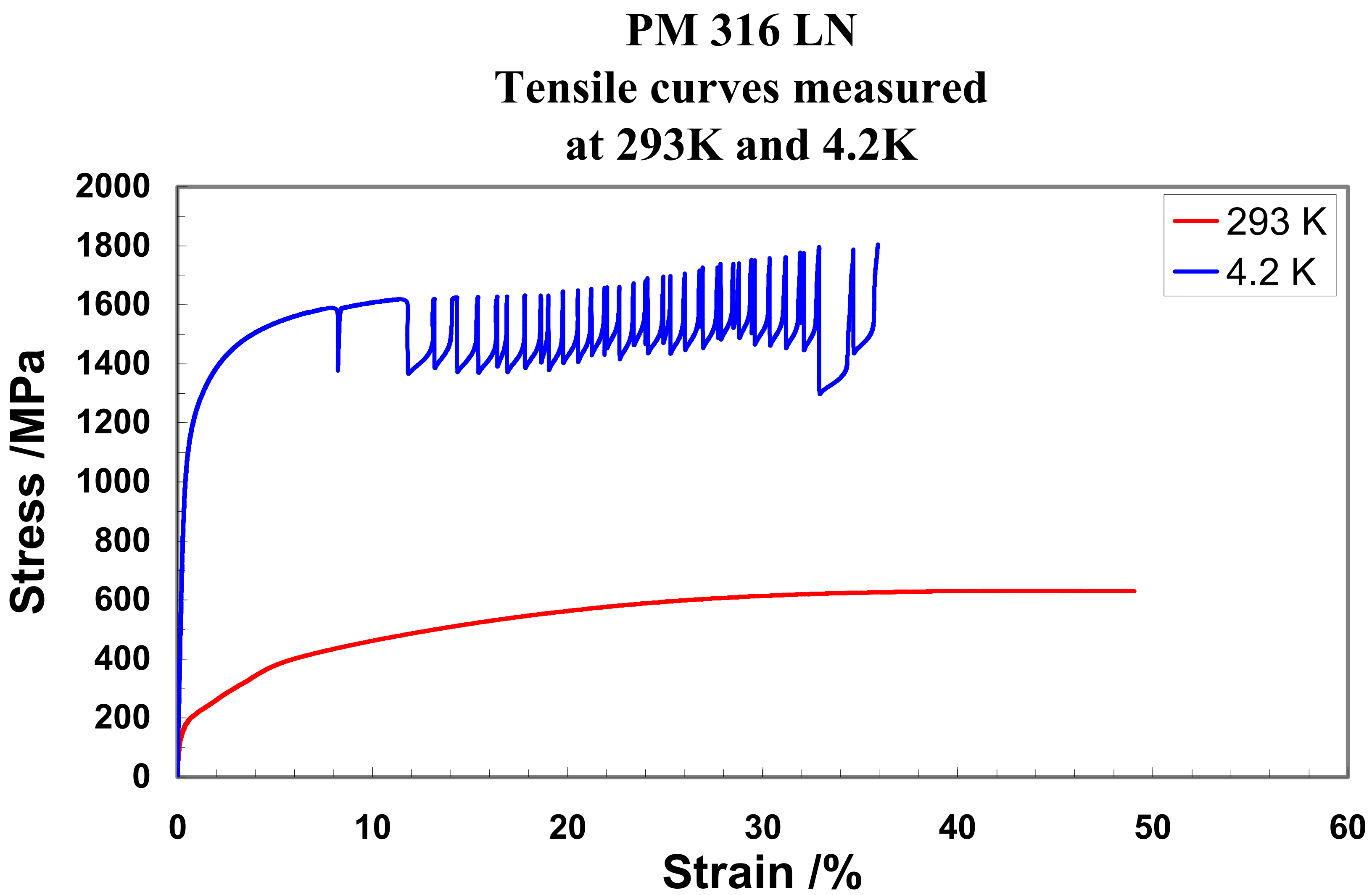

Compared tensile properties

of PM 316LN at 293 K and 4.2 K

of cast 316LN at 293 K and 4.2 K

of wrought 316LN at 293 K and 4.2 K

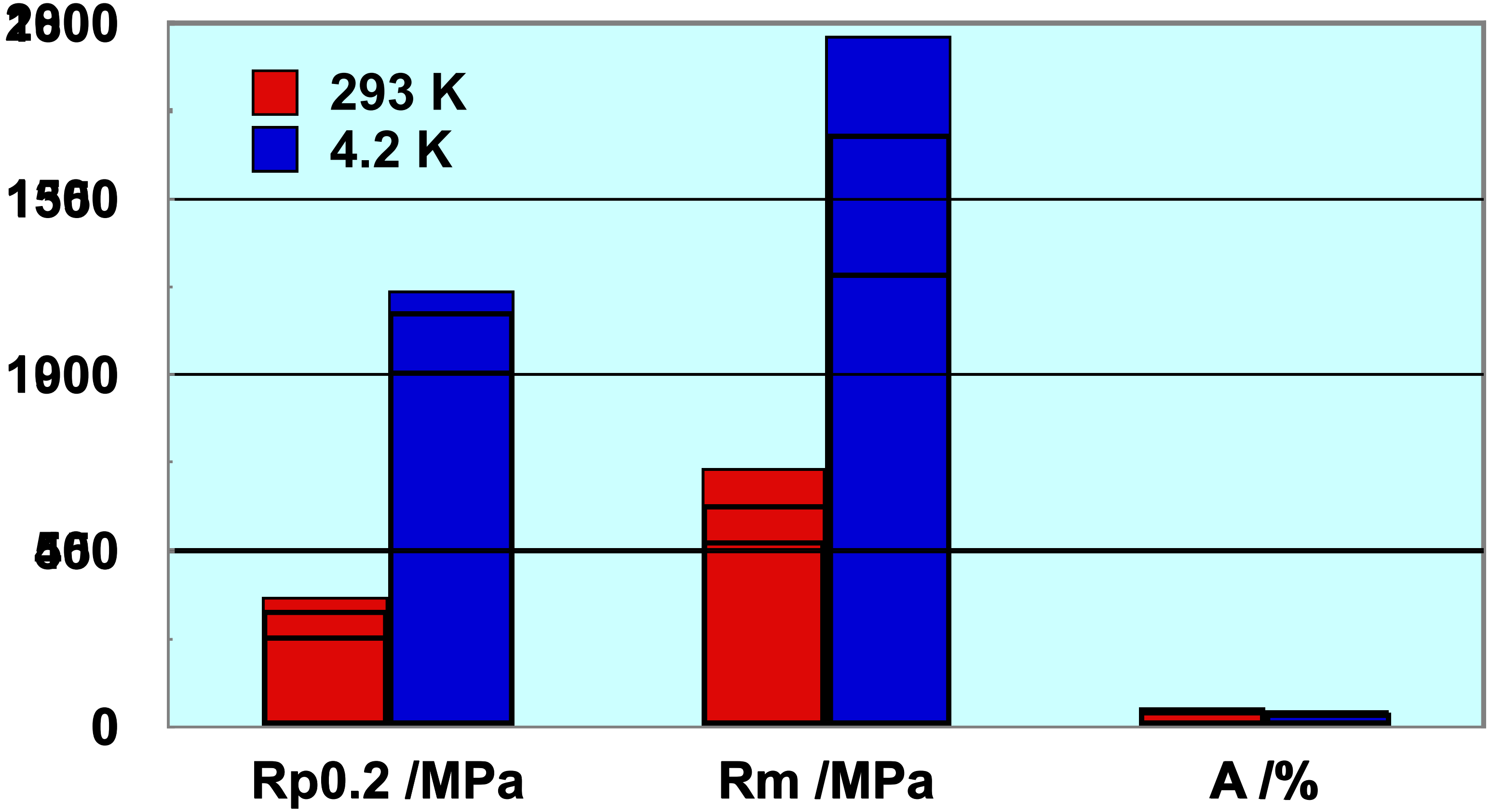

ISO-V impact energy at 4.2 K

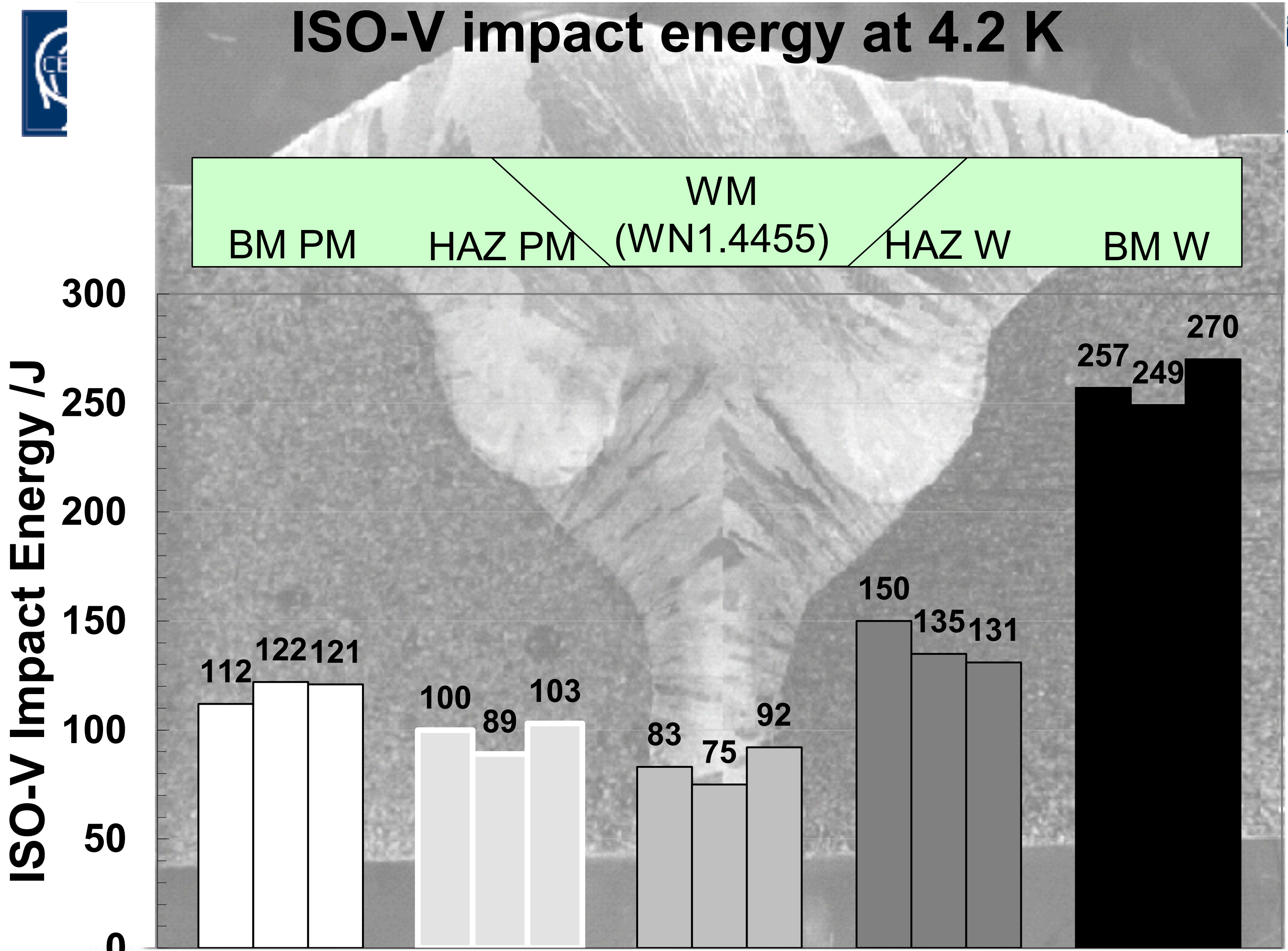

Fractographic analysis

Oxides within dimples

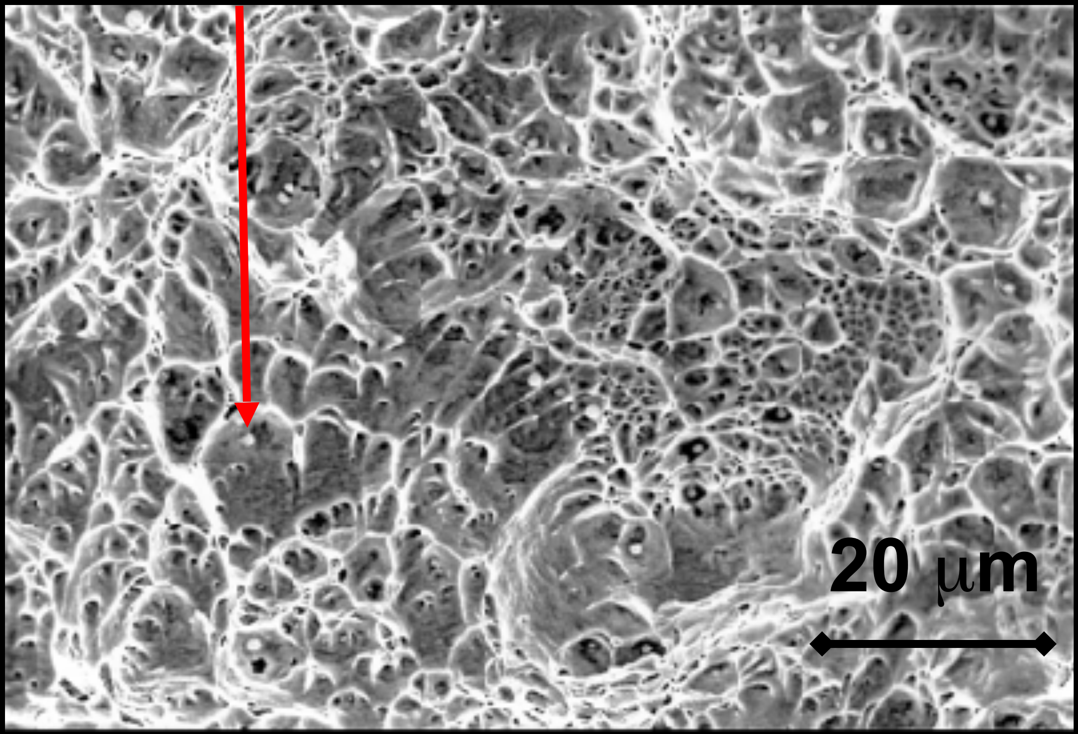

Localized ductility (Couturier 99)

HIPed PM 316LN		Metso	CERN Specification	
		H 6277	*Min.*	*Max.*
Composition (w%)	C	**0.017**		0.030
	Si	**0.59**		1.00
	Mn	**0.71**		2.00
	S	**0.005**		0.015
	P	**0.012**		0.040
	Ni	**13.07**	12.00	14.00
	Cr	**16.98**	16.00	18.00
	Mo	**2.53**	2.00	3.00
	O	**0.011**		
	N	**0.185**	0.15	0.20

Typical Oxygen levels

in 316LN:	Couturier et al. (1998)	**200 ppm**
	Dellis et al. (1996)	**195 ppm**
in 304L:	Appa Rao and Kumar. (1997)	**400 ppm**
in aust. SS	Zou and Grinder (1982)	**300 to 4500 ppm**
in 304L	Dunkley (1981)	**1200 to 7800 ppm**

Magnet end covers

Compared advantages of possible fabrication techniques

	welded	closed die forged	cast	PM
Microstructure	-	++	-	++
Tensile properties	+	+	-	++
Impact toughness at 4.2 K	+	++	+	+
Near net shaping	++	--	+	++
Reliability, NDT	--	++	--	++
Competitiviness, small series (tools)	+	--	+	+
Competitiviness, large series (tools)	+	+	+	+

PM Design Competition Award Winner

Award: Grand Prize
Year: 2007

Description:
The award was given to an end cover is used in the Large Hadron Collider, the world's largest and highest energy sub-atomic particle accelerator. Made from 316LN stainless steel powder, the part is hot isostatically pressed to full density. The superconducting dipole cryomagnets operate in a cryogenic environment at minus 450°F. As HIPed to a near-net shape of 253.5 pounds, the finished end cover weighs 153.3 pounds. The fabricator incorporated finite element analysis, computer aided design, numerically controlled sheet metal cutting technology, and cutting-edge robotic welding and part manipulation to produce the end covers. This resulted in a more-than-50-times increase over the typical production rate of fully-dense HIPed PM near-net shapes, an unprecedented breakthrough in productivity. About 2,700 end covers have been delivered to CERN. The design of the part features several complex configurations. For example, both the inner and outer surface of the broad face is radiused with the inner surface approximately parallel to the outer surface. The exterior of the curved surface has either eight or 10 projections, depending upon which version of the part is produced. The design differs slightly depending on which side of the dipole magnet it is located. The PM HIPed part meets the equivalent mechanical properties of 316LN wrought stainless steel, including internal toughness and high ductility.

Part: Dipole Cryomagnet End Cover
Fabricator: Bodycote HIP-Surahammar
End User: Metso Materials Technology Oy for CERN

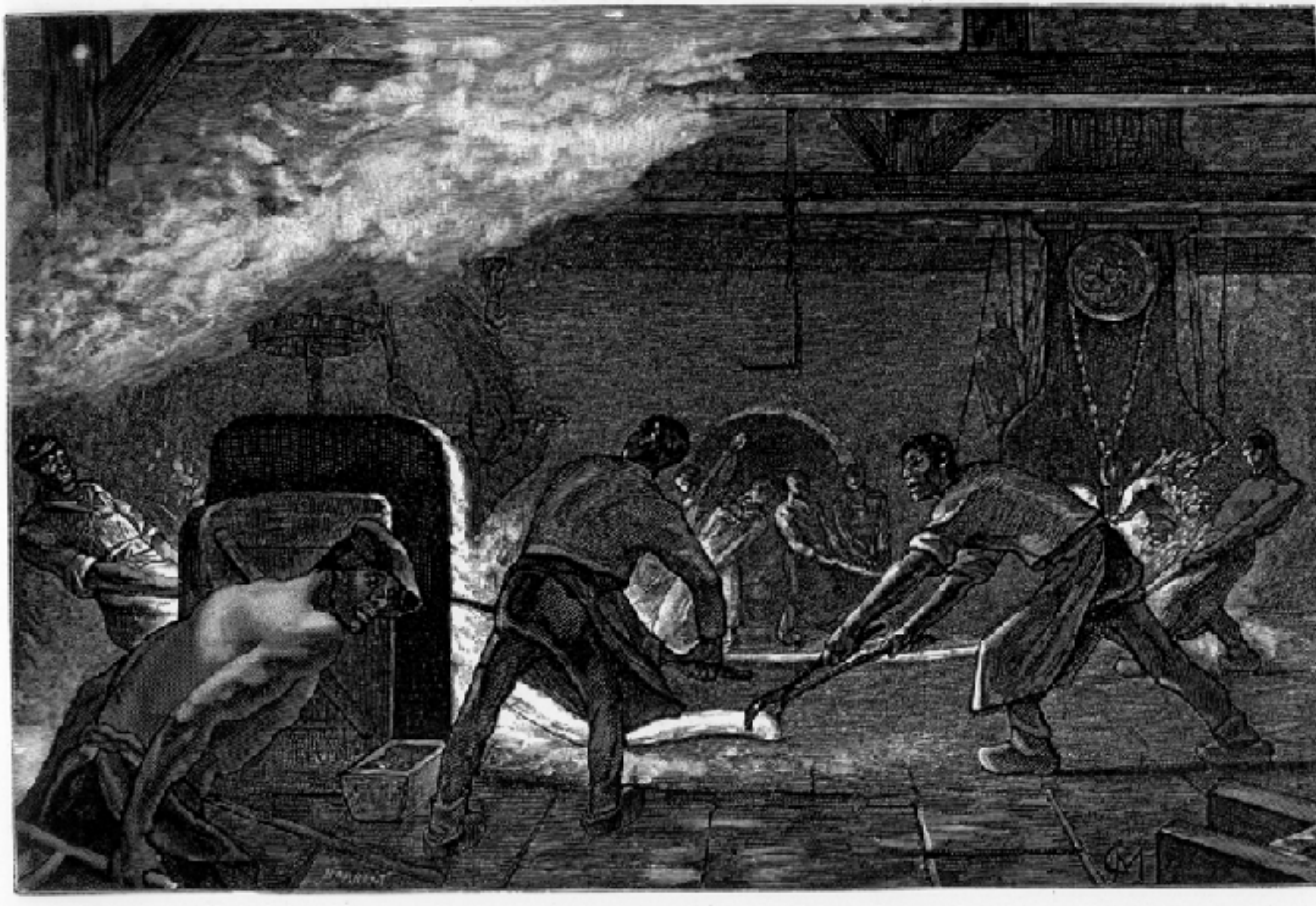

Dessin de Constantin Meunier.

TRAIN DE LAMINEURS DANS UN LAMINOIR DE MONTIGNY-SUR-SAMBRE.

General conclusions

(I) Conventional materials are key pieces of magnet technology (and of annual global market of magnetic materials) ⇒ selection, specification, purity, thermal treatments... require special care

(II) Soft ferromagnetic materials of better controlled properties/ metallurgy than constructional steels might be considered for specific applications (fast magnet systems...)

(III) Innovative materials of novel compositions, properties, metallurgy are relevant for an increasing number of applications to magnets

(IV) A selection of experimental methods reviewed, for soft ferromagnetic and feebly magnetic materials

(V) "Non-magnetic" ferrous materials deserve a critical selection

(VI) Importance and use of powder metallurgy is increasing for application to structural, soft magnetic materials and materials for permanent magnets

Concutiat motus, quis fulgura ducat hiatus,
Unde tonent nubes, quo lumine floreat arcus;
Hæc mihi quærenti, si quid deprendere veri
Mens valet, expediat. Lapis est cognomine Magnes,
Decolor, obscurus, vilis : non ille repexam
Cæsariem regum, nec candida virginis ornat
Colla, nec insigni splendet per cingula morsu :
Sed nova si nigri videas miracula saxi,
Tum pulchros superat cultus, et quidquid Eois
Indus litoribus rubra scrutatur in alga.

demens de la terre, et, déchirant la nue, en fait jaillir l'éclair, et fait gronder la foudre; quelle lumière colore l'arc d'Iris : moi aussi, je cherche à résoudre ces grands problèmes; et, si votre esprit peut entrevoir la vérité,

There is a stone called the magnet; black, dull, and common. It does not adorn the braided hair of kings nor the snowy necks of girls, nor yet shine in the jewelled buckles of warriors' belts. But consider the marvellous properties of this dull-looking stone and you will see that it is of more worth than lovely gems and any pearl sought of Indian amid the seaweed on the Red Sea's shores.

C. L. F. PANCKOUCKE.

Exegi monumentum ære perennius.
(Hor., Od. lib. III, od. 30.)

TOME SECOND

PARIS
C. L. F. PANCKOUCKE, EDITEUR
OFFICIER DE L'ORDRE ROYAL DE LA LÉGION D'HONNEUR,
RUE DES POITEVINS, N. 14
M DCCC XL